Bright Sirens: GRBs with known redshifts and facilities to detect them.

Anastasia Tsvetkova,

University of Cagliari,

KW team

History of GRB observations with Konuses

- One of the first independent confirmation of the GRB discovery. A gamma-ray detector on Kosmos-461 s/c detected GRB 720117 from the Vela catalog (Mazets et.al., JETP Letters 19, 126, 1974);
- ~150 GRBs were detected in the KONUS experiments on board Venera 11-14 missions in 1979-1983;
- Discovery of a bimodality in the GRB duration distribution and an isotropy of spatial distribution of their sources;

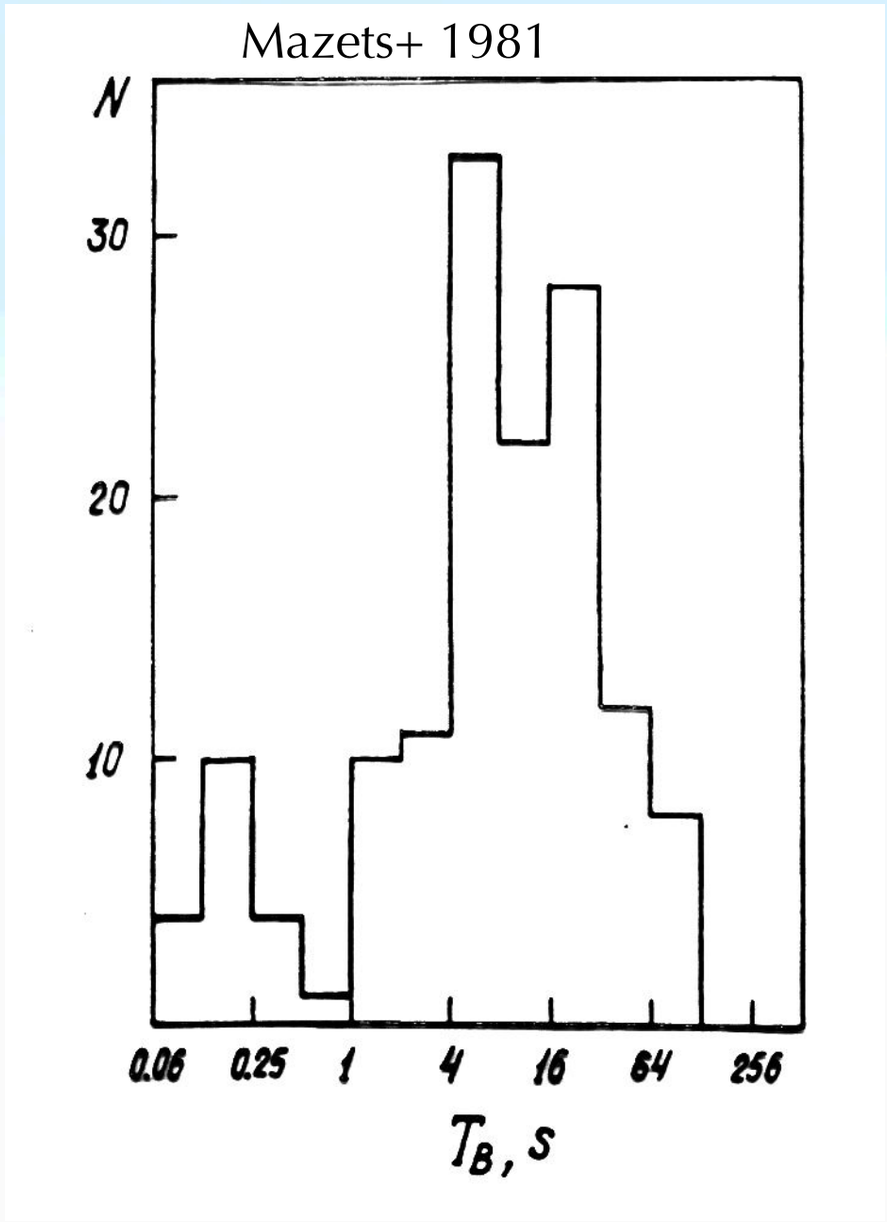

History of GRB observations with Konuses

- The first evidence of hardness-intensity correlations in GRBs (Venera 13-14 missions).

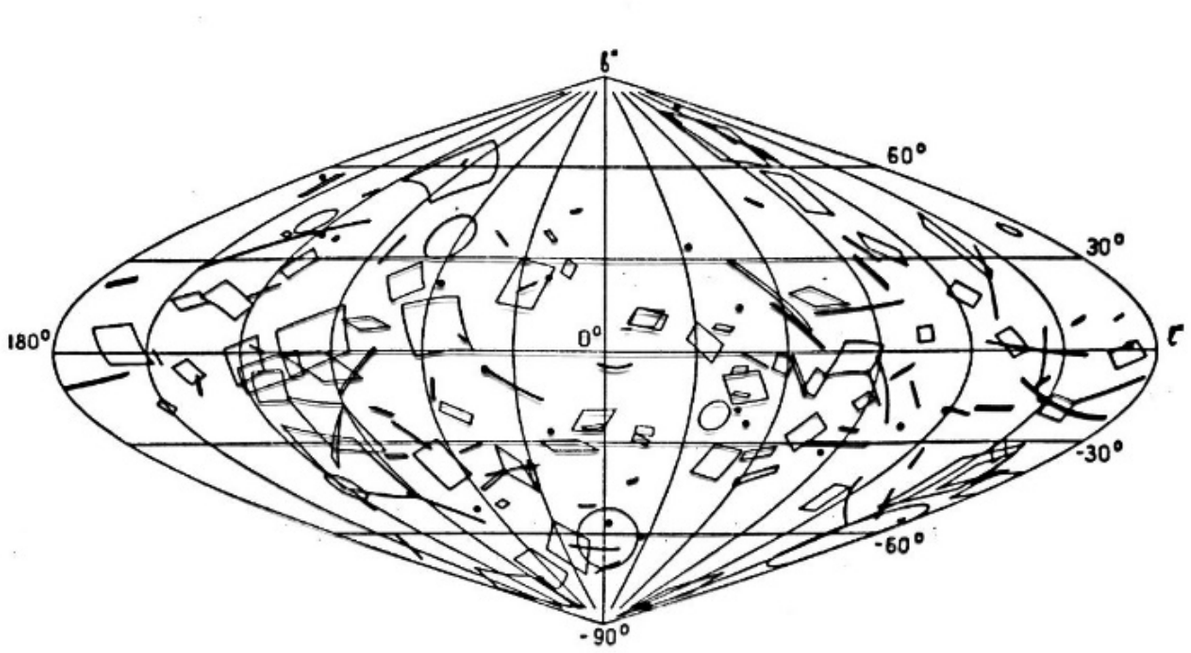

Mazets & Golenetskii, 1981

- The first evidence of hardness-intensity correlations in GRBs (Venera 13-14 missions).

Golenetskii+ 1983

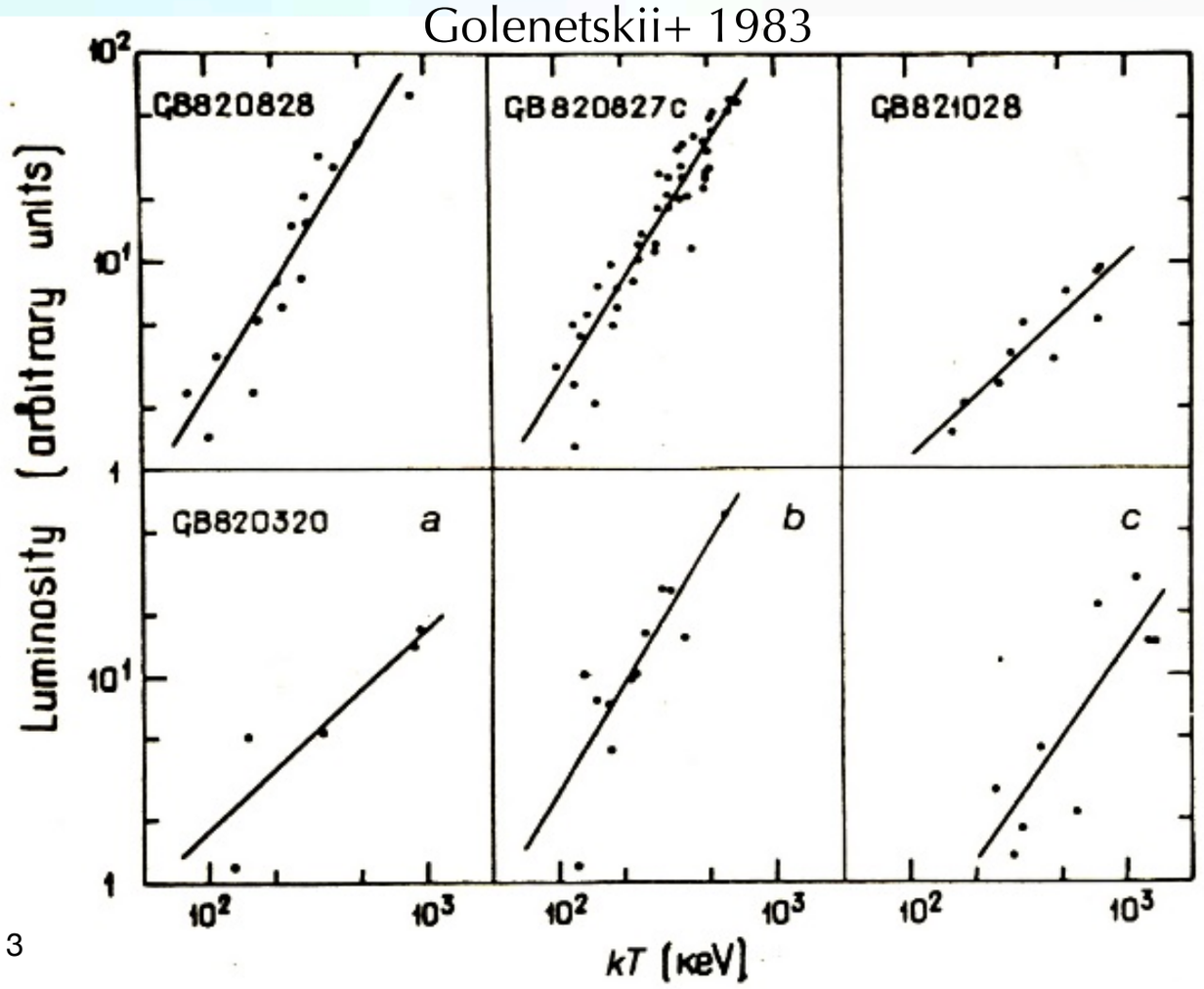

History of GRB observations with BATSE

- Eight modules (2 NaI ~51 cm in diameter and ~1.3 cm thick) operating in ~**10 keV–8 MeV** energy range;
- FoV ≈ 2.6π sr;
- Rough localisation;
- 5B catalog: **2145 GRBs**.

5 April 1991 — 4 June 2000

Breakthroughs in the field:

- Observation of the **sky and intensity distribution** of numerous GRBs provided strong evidence for the cosmological distances to them;
- Definitive separation between the **short/hard** and the **long/soft** classes of GRBs;
- Evidence that many GRB spectra are nicely fit by the Band function;
- "Hard-to-soft" evolution of GRB spectra.

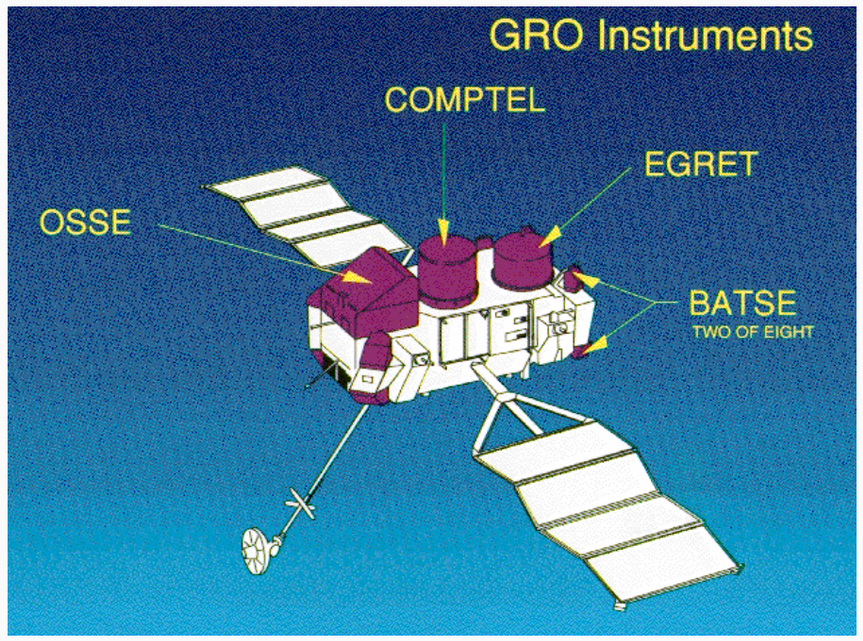

History of GRB observations with BeppoSAX

April 30, 1996 —April 30, 2002

Breakthroughs in the field:

- The first rapid **arcmin localization** and first X-ray **follow-up** observations of GRB 970228 (host galaxy);
- The first direct **redshift** measurements of the optical afterglow of GRB 970508 with ground-based telescopes;
- The **GRB/SN connection**;
- The existence of a **hardness–intensity correlation** of GRB prompt emission in the rest frame.

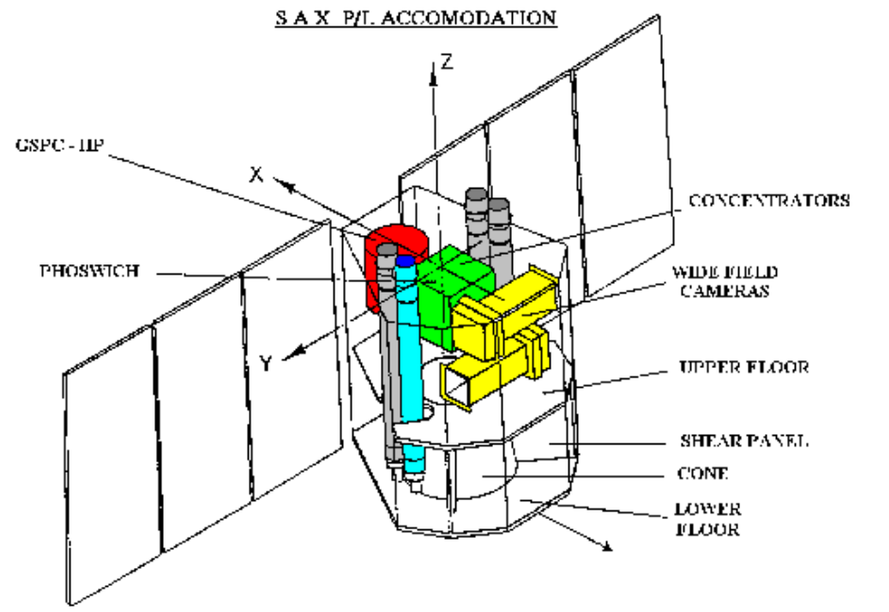

Instrument overview

Mission	Operation Period	Instrument	Energy Range	Localization Accuracy
Venera 11–14	1979–1983	Konus	20 keV–2 MeV	$\gtrsim 10°$
CGRO	1991–2000	BATSE EGRET	20 keV–2 MeV 20 MeV–30 GeV	$\gtrsim$few deg
Wind	1994–present	Konus-Wind	20 keV–20 MeV	
BeppoSAX	1996–2002	GRBM WFC NFIs	40–700 keV 2–26 keV 0.1–300 keV	1–3′
CXO	1999–present	ACIS	0.5–8 keV	$\lesssim 1''$
XMM-Newton	1999–present	EPIC	0.1–15 keV	$\lesssim 2''$
HETE-2	2000–2006	FREGATE WXM SXC	6–400 keV 2–25 keV 0.5–10 keV	3–15″
INTEGRAL	2002–present	SPI/ACS IBIS	20 keV–8 MeV 15 keV–10 MeV	10–20′ <1′

Instrument overview

Swift	2004–present	BAT XRT UVOT	15–150 keV 0.2–10 keV 170–650 nm	1–3′ 3″ 0.3″
Suzaku	2005–2015	WAM	50-5000 keV	5°–10°
AGILE	2007–present	GRID SA	30 MeV–50 GeV 15–45 keV	5–20′ 1–3′
Fermi	2008–present	LAT GBM	20 MeV– $\gtrsim$300 GeV 8 keV–40 MeV	0.2–0.5° $\gtrsim$few deg
MAXI	2009–present	GSC SSC	2–30 keV 0.5–10 keV	$<6'$ $<6'$
IKAROS	2010–2015	GAP	50–300 keV	
NuSTAR	2012–present		3–79 keV	
AstroSAT	2015–present	SZTI	10–100 keV	
CALET	2015–present	CGBM	7 keV–20 MeV	

Instrument overview

Mission	Operation Period	Instrument	Energy Range	Localization Accuracy
Lomonosov	2016–2019	BDRG	10–3000 keV	$\gtrsim$few deg
		SHOK	330–820 nm	
		UBAT	5–200 keV	
		SMT	200–650 nm	0.5″
Polar	2016–2017		50–500 keV	
Insight-HXMT	2017–present	HE	40 keV–3 MeV	
ASIM	2018–present	MXGS	20 keV– >20 MeV	
GECAM	2020–present		6 keV–5 MeV	$\gtrsim$few deg
SVOM	2023	ECLAIRs	4–250 keV	>12′
		GRM	15 keV–5 MeV	
		MXT	0.2–10 keV	1′
		VT	450–1000 nm	<1″
Einstein Probe	2023	WXT	0.5–4.0 keV	< 1′
		FXT	0.5–4.0 keV	<10″

THESEUS

Mission	Autonomous rapid repointing	Arcsec localisation	Optical imaging	Near-IR imaging	Near-IR spectroscopy	On-board redshift broadcasting	<10 keV X-ray coverage	>10 keV X-ray coverage	MeV γ-ray coverage
Swift	✓	✓	✓	×	×	×	✓	✓	×
Fermi/GRB	×	×	×	×	×	×	×	✓	✓
Integral	×	×	✓	×	×	×	×	✓	✓
SVOM	✓	✓	✓	×	×	×	✓	✓	✓
Einstein Probe	✓	×	×	×	×	×	✓	×	×
eXTP	✓	✓	×	×	×	×	✓	×	×
THESEUS	✓	✓	✓	✓	✓	✓	✓	✓	✓

Payload:

- Soft X-ray Imager (SXI, 0.3 – 5 keV): a set of 2 lobster-eye telescopes units, covering a total field of view (FOV) of ~0.5sr with source location accuracy < 1–2′;
- InfraRed Telescope (IRT, 0.7 – 1.8 μm): a 0.7m class IR telescope with 15′x15′ FOV, for fast response, with both imaging and spectroscopy capabilities;
- X-Gamma rays Imaging Spectrometer (XGIS, 2 keV – 20 MeV): a set of 2 coded-mask cameras using monolithic X-gamma rays detectors based on bars of Silicon diodes coupled with CsI crystal scintillator, granting a ~2sr FOV and a source location accuracy of ~10 arcmin in the 2–150 keV, as well as a >4sr FoV at energies >150 keV.

THESEUS: scientific objectives

Amati+ (2015)

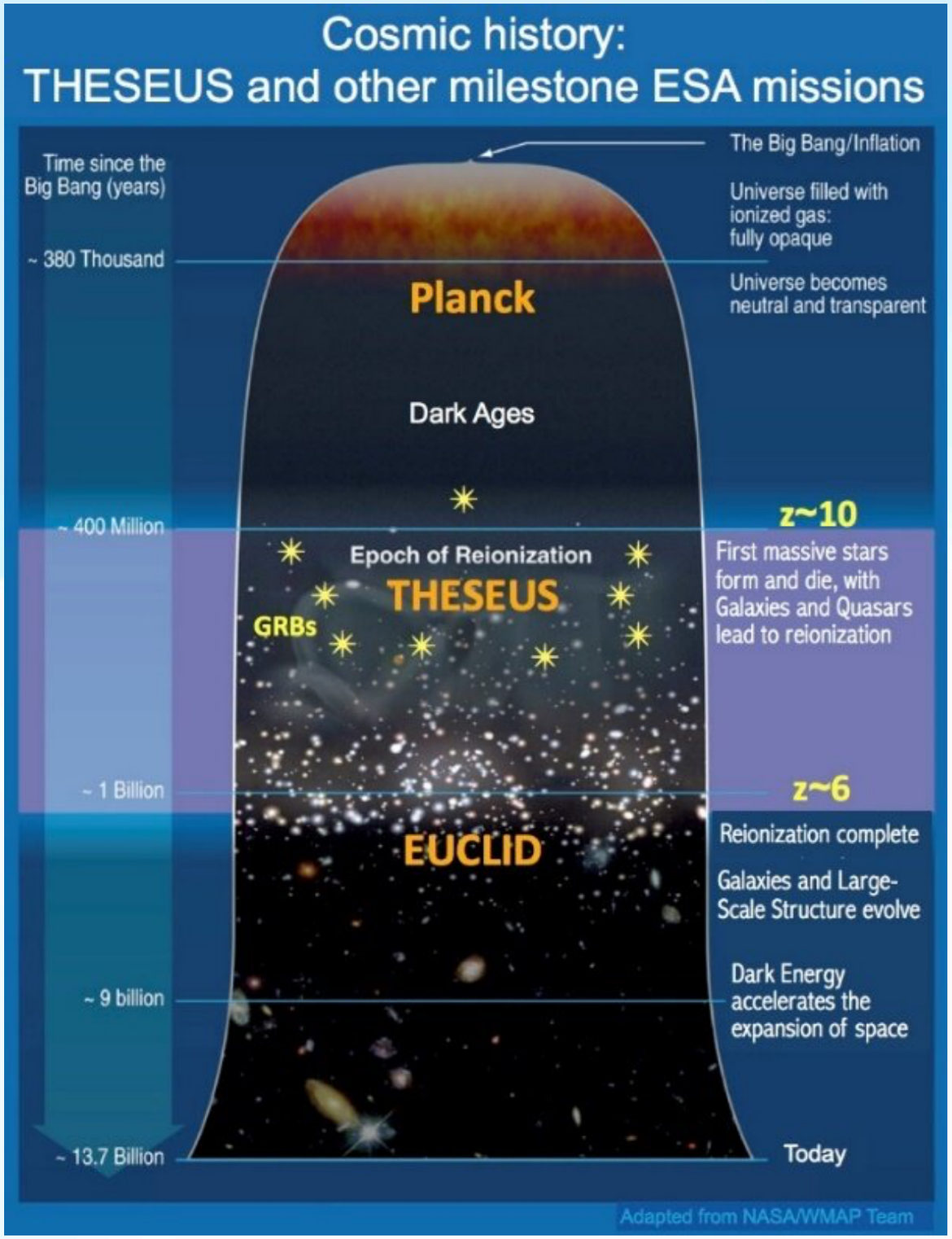

1. Explore the cosmic dawn and reionization era:

- Low-luminosity primordial galaxies;
- Global star formation history of the Universe up to z~10;
- Reionization epoch, ISM and IGM up to z~6–10 => how reionization proceeded as a function of environment, if radiation from massive stars was its primary driver and how did cosmic chemical evolution proceed as a function of time and environment;
- When the first stars formed and how did the earliest Pop III and Pop II stars influence their environment.

THESEUS: scientific objectives

2. **Provide key observations for multi-messenger and time-domain astrophysics:**

- Locate and identify the electromagnetic counterparts to sources of GW and ν;
- Provide real-time triggers and accurate (≤15′ within a few seconds; ~1″ within a few minutes) **positions of GRBs**;
- Give fundamental insights into the physics and progenitors of **GRBs and cc-SN connection;**
- **Sub-energetic** GRBs and X-Ray Flashes;
- Physics of **Galactic and extra-Galactic transients**, e.g., TDEs, magnetars / SGRs, SNe shock break-outs, Soft and Hard X-ray Transients, thermonuclear bursts from accreting NS, novae, dwarf novae, stellar flares, AGN) and blazars.

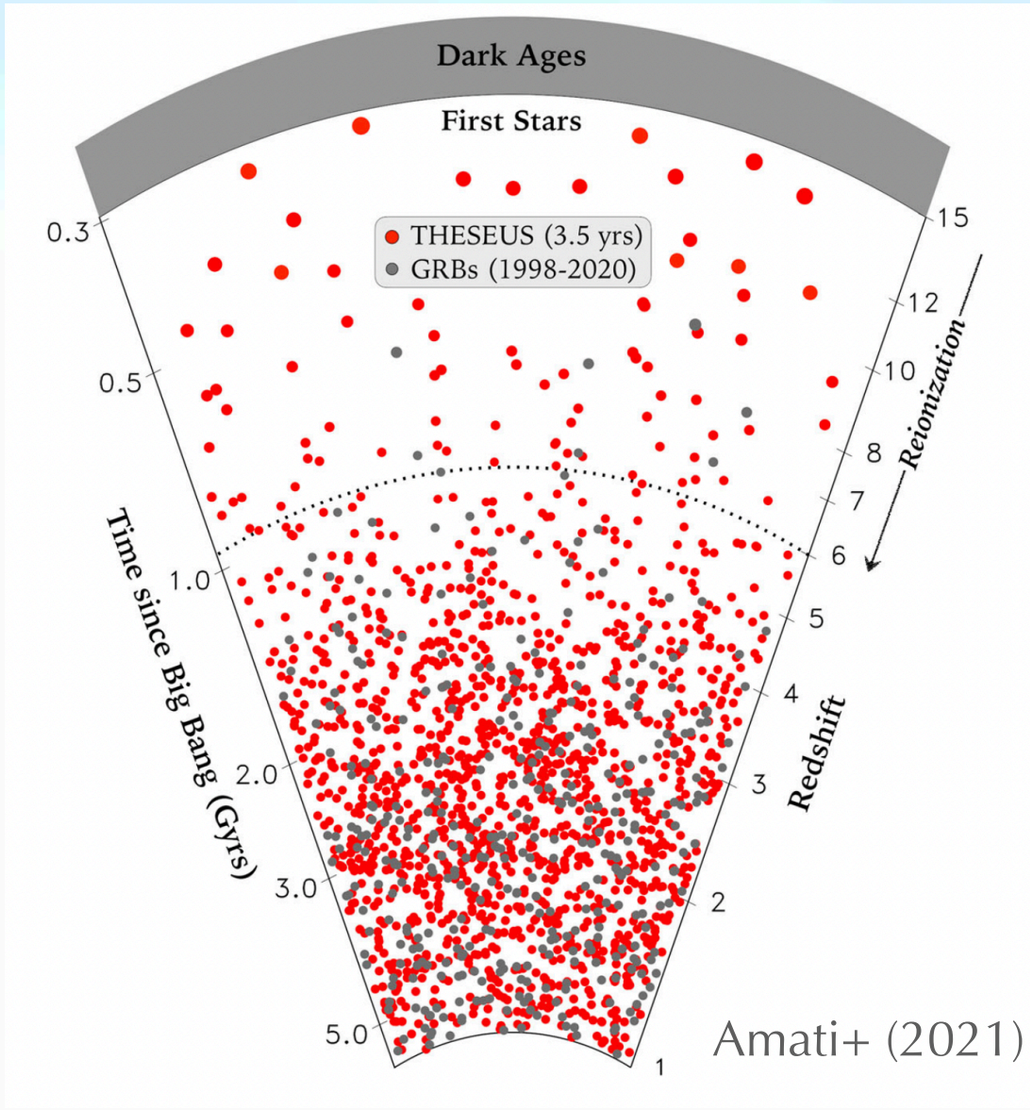

Einstein Probe

Instruments:

1. Wide-field X-ray Telescope (**WXT**): 12 Lobster-eye optics sensor modules, together creating a very large instantaneous **FoV of 3600 deg²**.

- The nominal detection bandpass of WXT is **0.5–4.0 keV**.

2. Follow-up X-ray Telescope (**FXT**): FXT has optics adopted from eROSITA, "the mirror module consists of 54 nested Wolter mirrors with a focal length of 1600 mm and an **effective area of >300 cm² at 1.5 keV**.

- Operates in the **0.5–10 keV** energy range.
- It has a narrow **FoV of 60 arcmin** in diameter and a source localization error of **5–15 arcsec** (90% c.l.).

Launch: 9 Jan 2024

Scientific objectives:

- Identify inactive black holes to study how matter is precipitated there by detecting the transient events that take the form of X-ray flares;
- Detect the electromagnetic counterparts of GW events;
- Permanent monitoring of the entire sky to detect the various transients and carry out measurements of known variable X-ray sources.

BeppoSAX/WFC

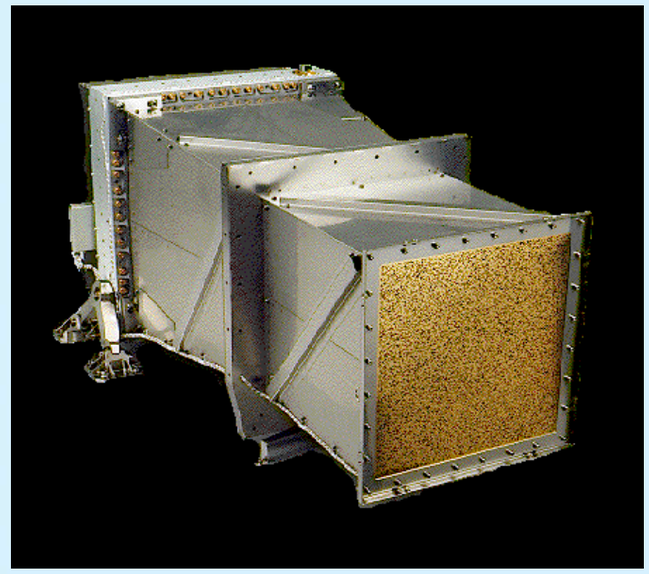

April 30, 1996 —April 30, 2002

- Two coded aperture cameras operating in the **1.8–28 keV** range and each covering a region of **40º x 40º** on the sky;
- Spectral resolution: **20% at 6 keV** (FWHM);
- Time resolution: **0.5 ms**;
- Effective area ~**138 cm²** at 10.5 keV;
- The source location accuracy for bright sources: **1.4′** at 99% CL;
- The on-axis sensitivity was in the range 2–10 mCrab for a typical BeppoSAX WFC observation of 3×10^4 s.

Scientific goals:

- Monitor large but selected regions of the sky for cosmic X-ray transient sources and signal the necessity for **follow-up studies** with higher-sensitivity narrow-field instruments on BeppoSAX and other platforms;
- Perform spatially-resolved simultaneous monitoring of compact **X-ray sources** in crowded fields with high sensitivity

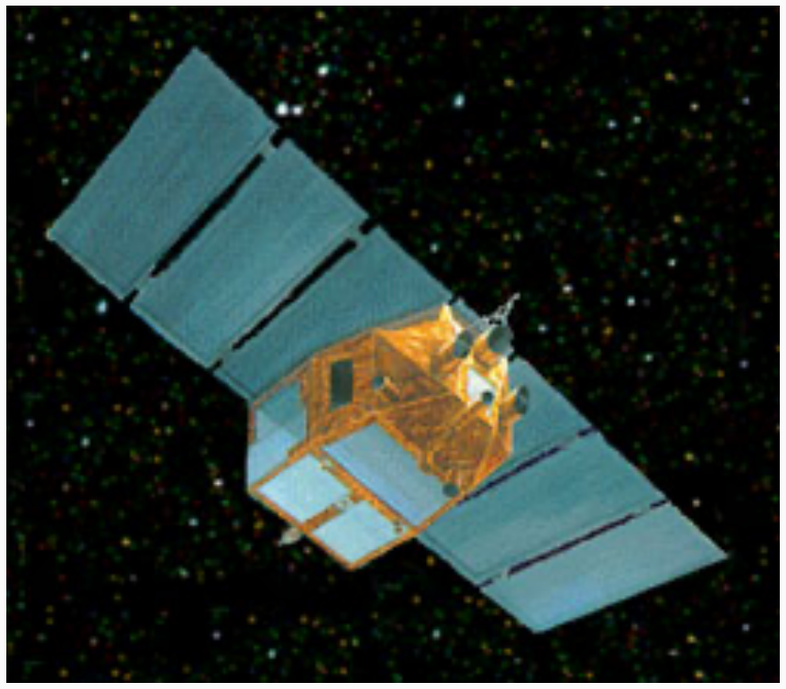

Key space and ground facilities in GRB science

Tsvetkova+ 2022

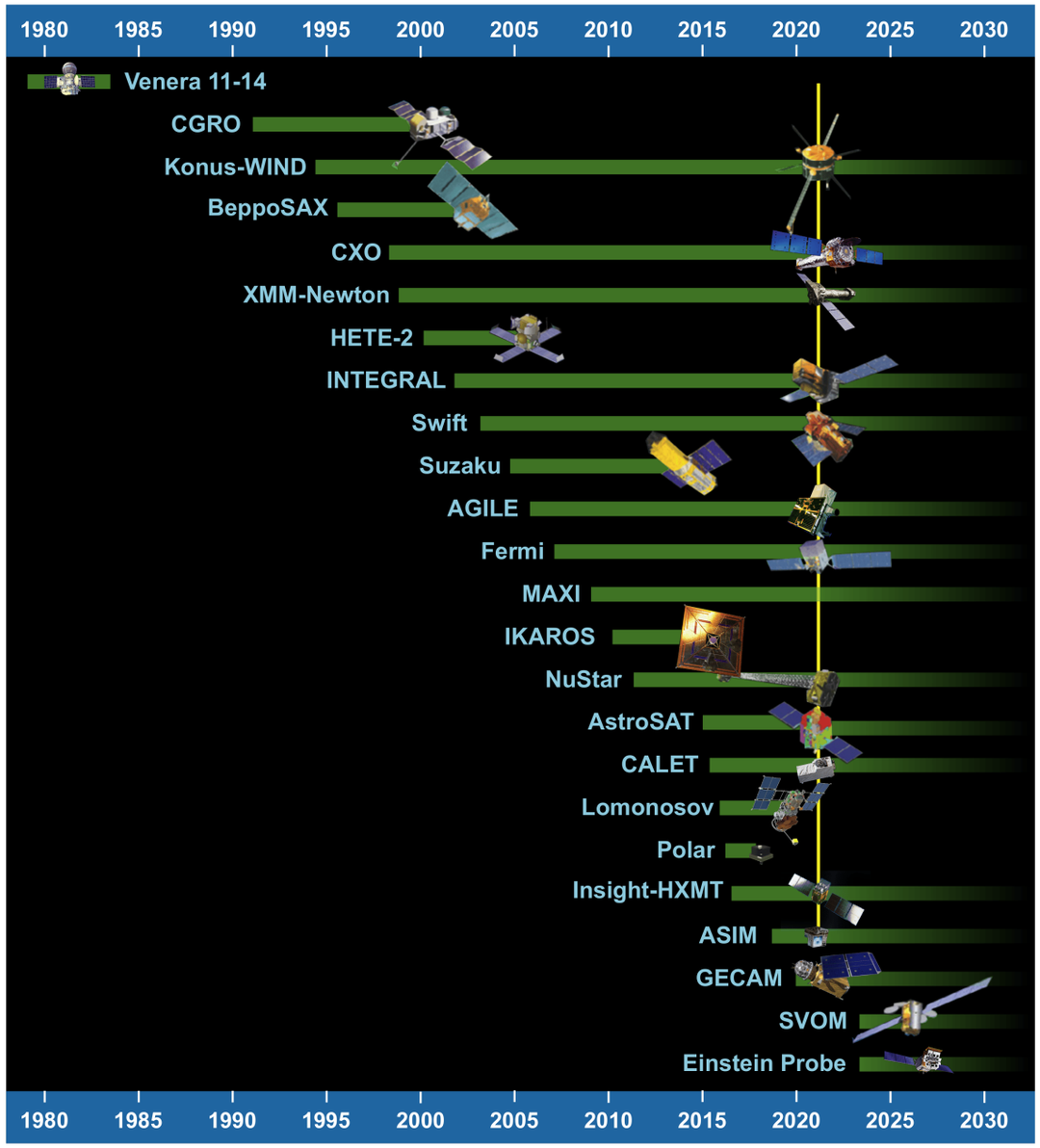

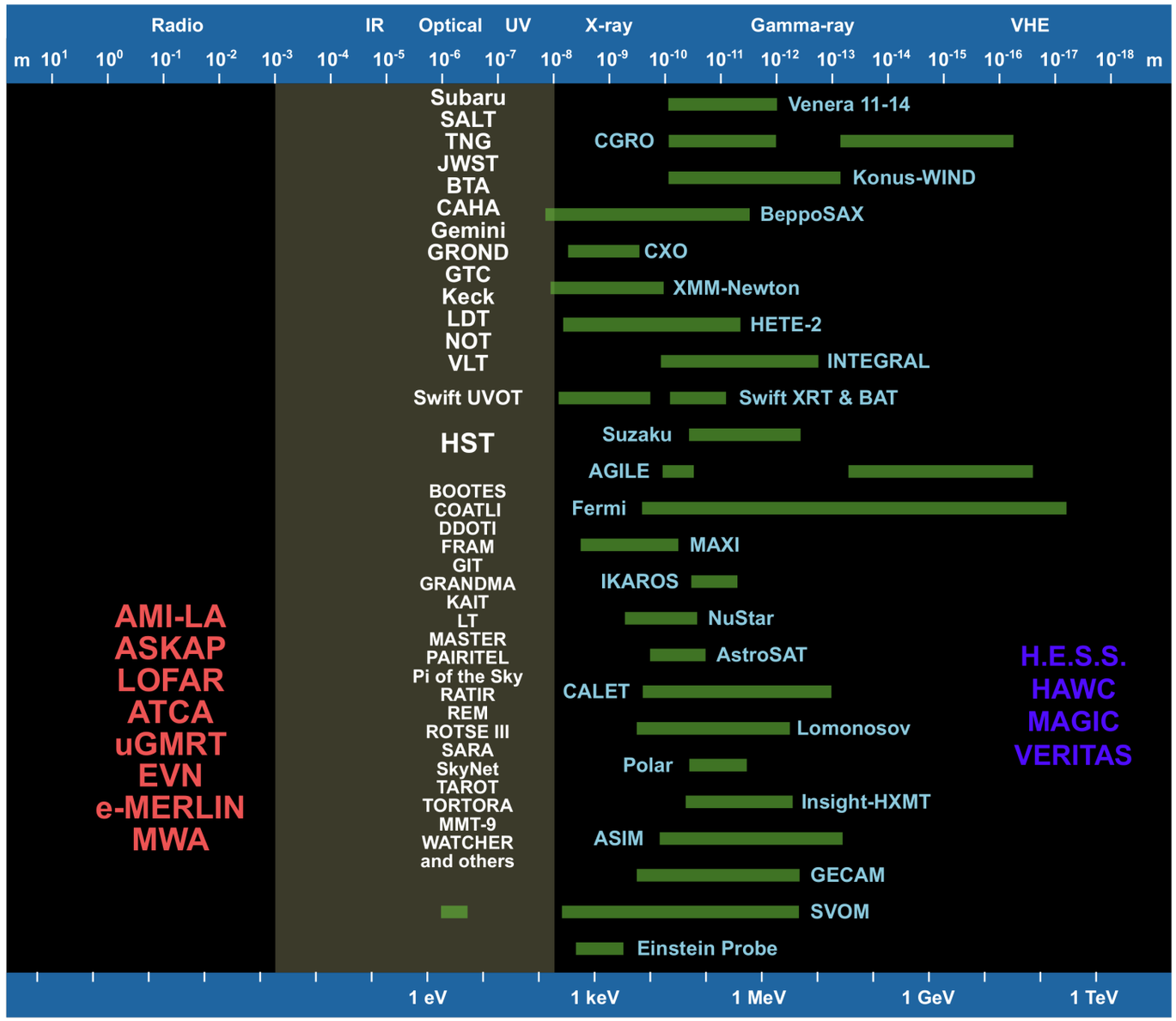

Key space and ground facilities in GRB science

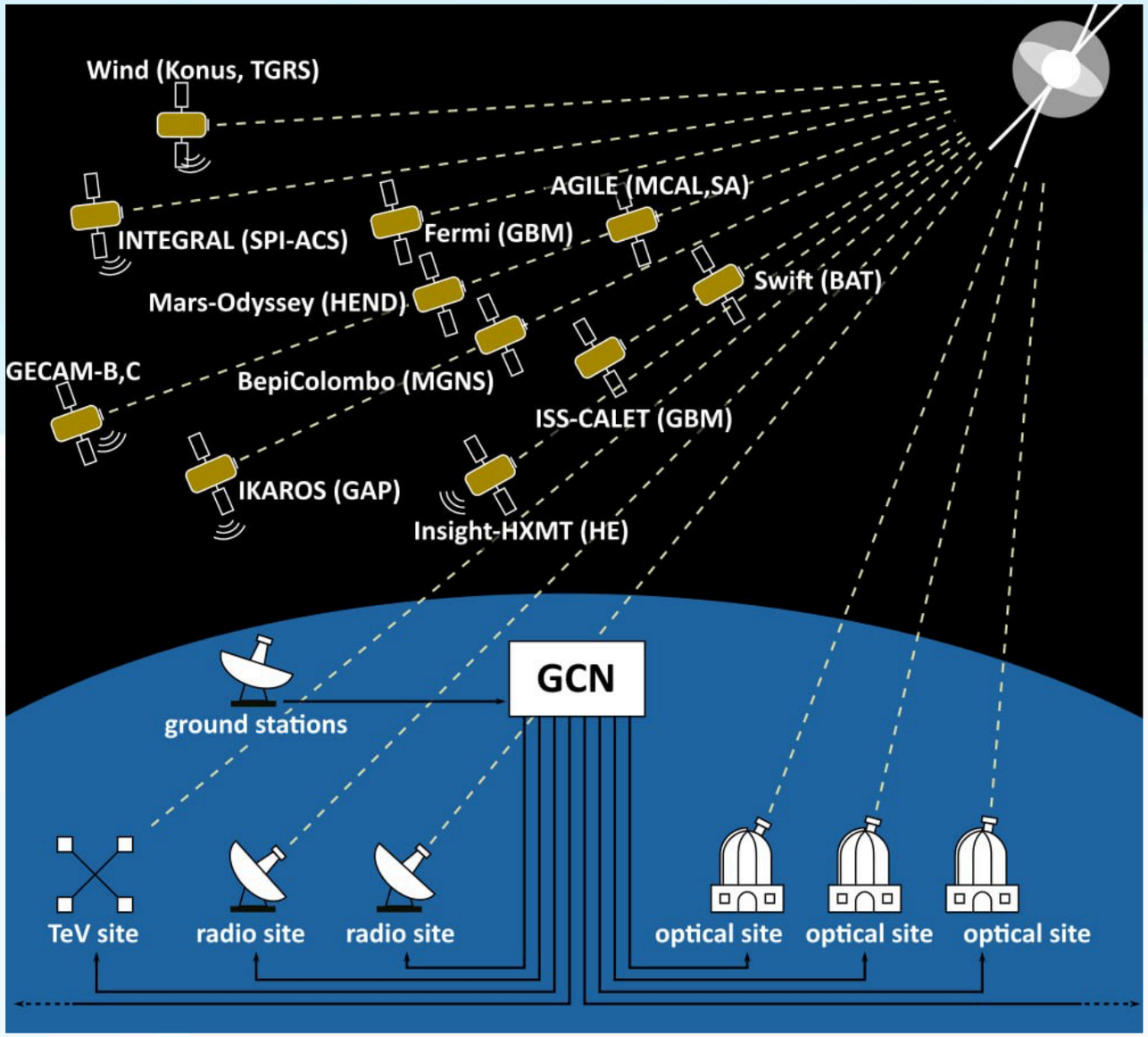

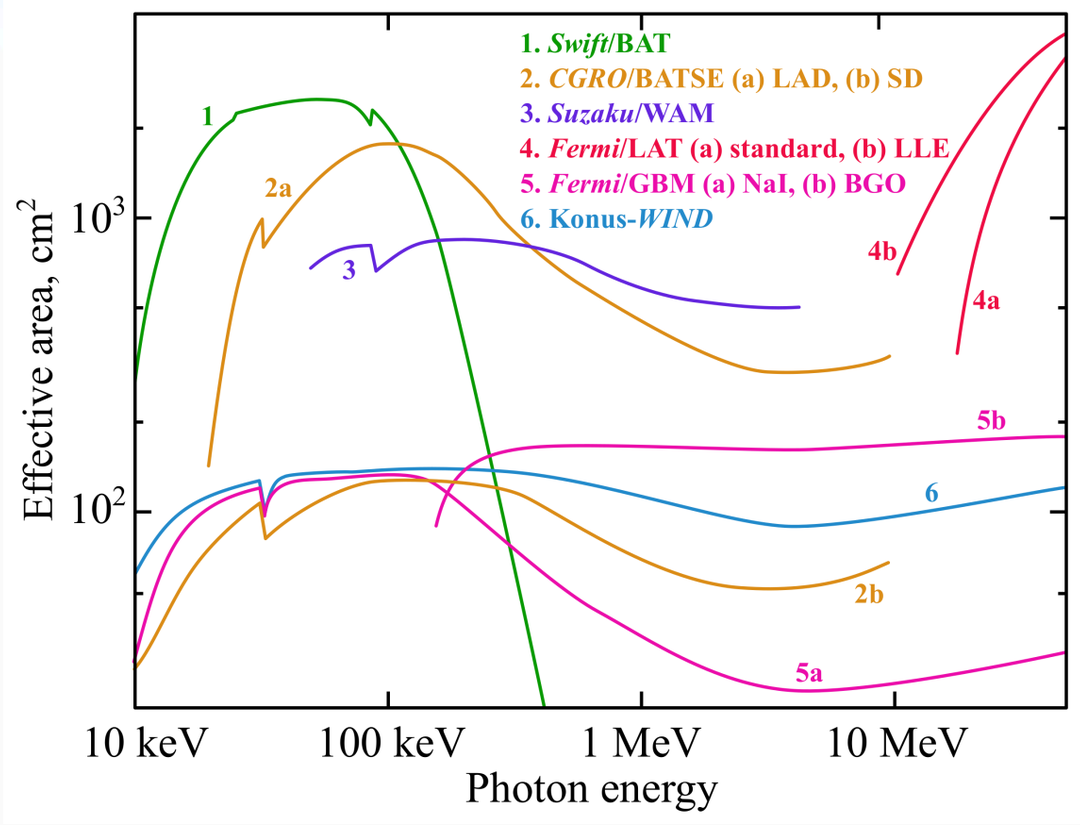

Key space and ground facilities in GRB science

universe

MDPI

Review

Key Space and Ground Facilities in GRB Science

Anastasia Tsvetkova [1,2,*], Dmitry Svinkin [1], Sergey Karpov [3,4,5] and Dmitry Frederiks [1]

[1] Ioffe Institute, Politekhnicheskaya 26, 194021 St. Petersburg, Russia; svinkin@mail.ioffe.ru (D.S.); fred@mail.ioffe.ru (D.F.)
[2] Dipartimento di Fisica, Università degli Studi di Cagliari, SP Monserrato-Sestu, km 0.7, I-09042 Monserrato, Italy
[3] CEICO, Institute of Physics, Czech Academy of Sciences, 182 21 Prague, Czech Republic; karpov@fzu.cz
[4] Special Astrophysical Observatory, Russian Academy of Sciences, 369167 Nizhniy Arkhyz, Russia
[5] Institute of Physics, Kazan Federal University, 420008 Kazan, Russia
* Correspondence: tsvetkova@mail.ioffe.ru or tsvetkova.lea@gmail.com

Abstract: Gamma-ray bursts (GRBs) are short and intense flashes of γ-rays coming from deep space. GRBs were discovered more than a half century ago and now are observed across the whole electromagnetic spectrum from radio to very-high-energy gamma rays. They carry information about the powerful energy release during the final stage of stellar evolution, as well as properties of matter on the way to the observer. At present, space-based observatories detect on average approximately one GRB per day. In this review, we summarize key space and ground facilities that contribute to the GRB studies.

Keywords: gamma-ray bursts; instrumentation; detectors

Konus-*Wind* experiment

- The Konus-Wind (KW) is aimed primarily at GRB and SGR studies;
- Launched on November 1, 1994: almost 30 years of continuous operation;
- Now in orbit near L1, up to 2.1×10^6 km (~7 light s) from Earth;
- The first Russian scientific instrument onboard an American satellite;
- Observation statistics (triggers): 5600 - total, 3800 – GRBs (Fermi ~3800, BATSE ~2100, Swift ~1600), 320 – SGRs, 1200 – SFs.

Advantages

- Wide energy band;
- Exceptionally stable background;
- The orbit of s/c excepts interferences from radiation belts and the Earth occultation;
- Continuous observations of all sky;
- Duty cycle 95%;
- Observes almost all bright events ($>10^{-6}$ erg cm^{-2} s^{-1}).

Konus-Wind, Swift-BAT, and Fermi-GBM properties

	KW	BAT	GBM
Crystal	NaI(Tl)	CdZnTe	NaI(Tl)/BGO
Number of detectors	2	– [a]	12/2
Diameter (cm)	12.7	–	12.7/12.7
Thickness(cm)	7.5	–	1.27/12.7
Approx. max. eff. area (cm^2)	160	5200	120/110
Energy range	20 keV–20 MeV [b]	14–150 keV [c]	8 keV–40 MeV
Approx. sensitivity (erg cm^{-2} s^{-1})	5×10^{-7}	1×10^{-8}	5×10^{-8}
FoV (sr)	4π	1.4 [d]	> 8
Operation time (yrs)	27	17	13
SGRB-to-LGRB rate	1:5	1:9	1:5

[a]: BAT is an assembly of 32,768 planar CdZnTe detectors (4×4 mm^2 large, 2 mm thick) to form a 1.2 m $\times$ 0.6 m sensitive area; [b]: Drifts with time; [c]: For coded FoV and up to 350 keV with no position information; [d]: For >50% coded FoV; ~2.2 sr for >10% coded FoV.

Konus-*Wind* experiment

Two observation modes

Triggered

- LCs in three energy windows G1, G2, and G3 (20 – 1200 keV) with the 2 - 256 ms time res. collected from T0-0.512 s to T0+230 s;
- Spectral data: 64 ch x 2 PHA (20 keV – 20 MeV) in 64 time bins with the 64 ms - 8 s time resolution lasting up to ~79–492 s.

Waiting

- LCs in three energy windows G1, G2, and G3 with ~ 3 s time res.
- 3-ch spectral data in G1, G2, G3

- G1 (~20–80 keV);
- G2 (~80–300 keV)
- G3 (~300–1200 keV)

KW GRBs with z: Triggered sample

- 150 (193 up to now) GRBs
- $0.1 \leq z \leq 5$
- 12 (14) Type I GRBs, 158 Type II GRBs
- 32 GRBs have reliable jet breaks times collimation factor

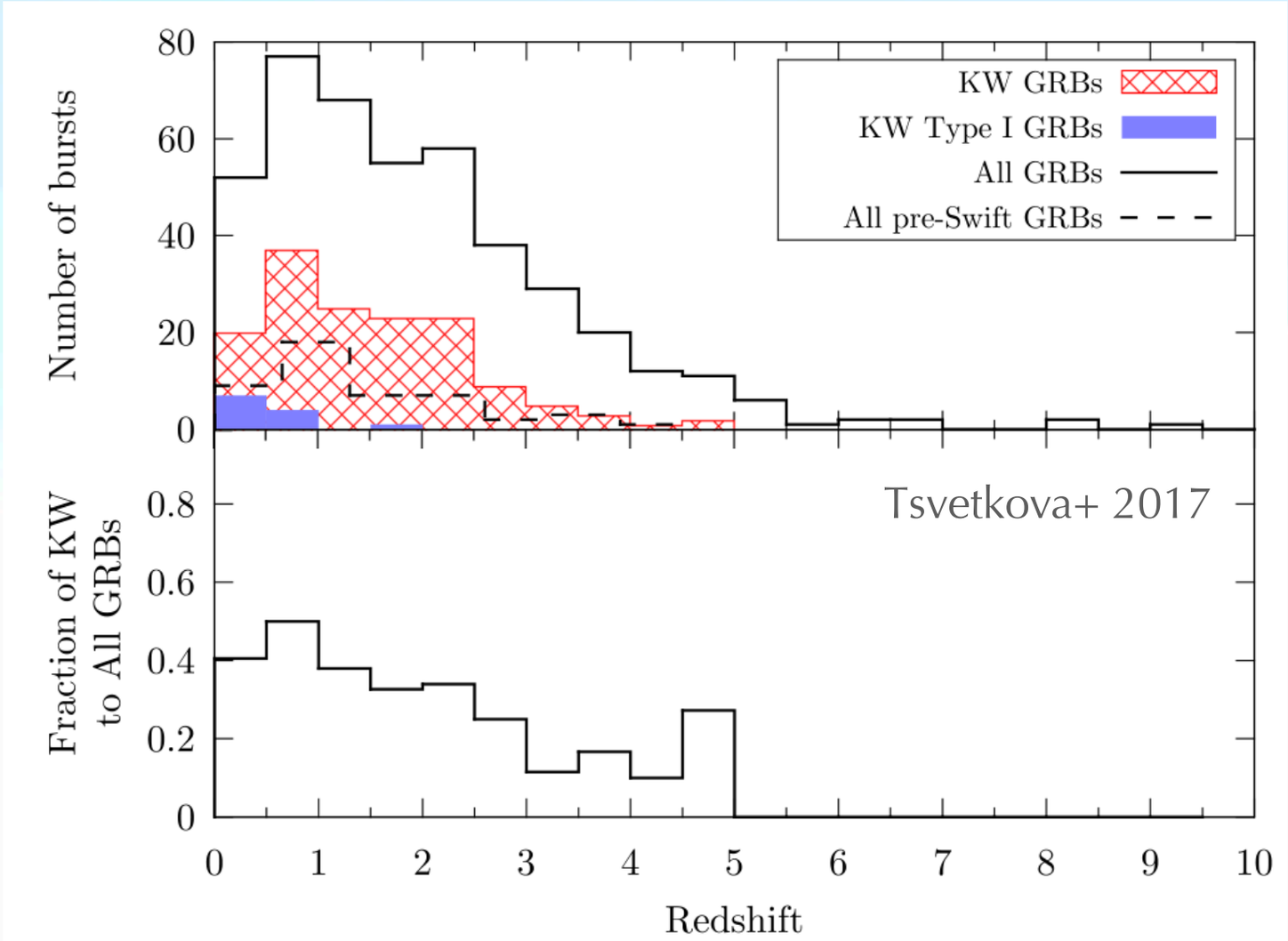

KW GRBs with z: Non-triggered sample

- 167 weak soft GRBs detected simultaneously with Swift/BAT (up to the end of 2018)
- 14 GRBs with reliable jet break times
- All peak energies constrained
- Four SGRBs and three XRFs
- $0.04 \leq z \leq 9.4$

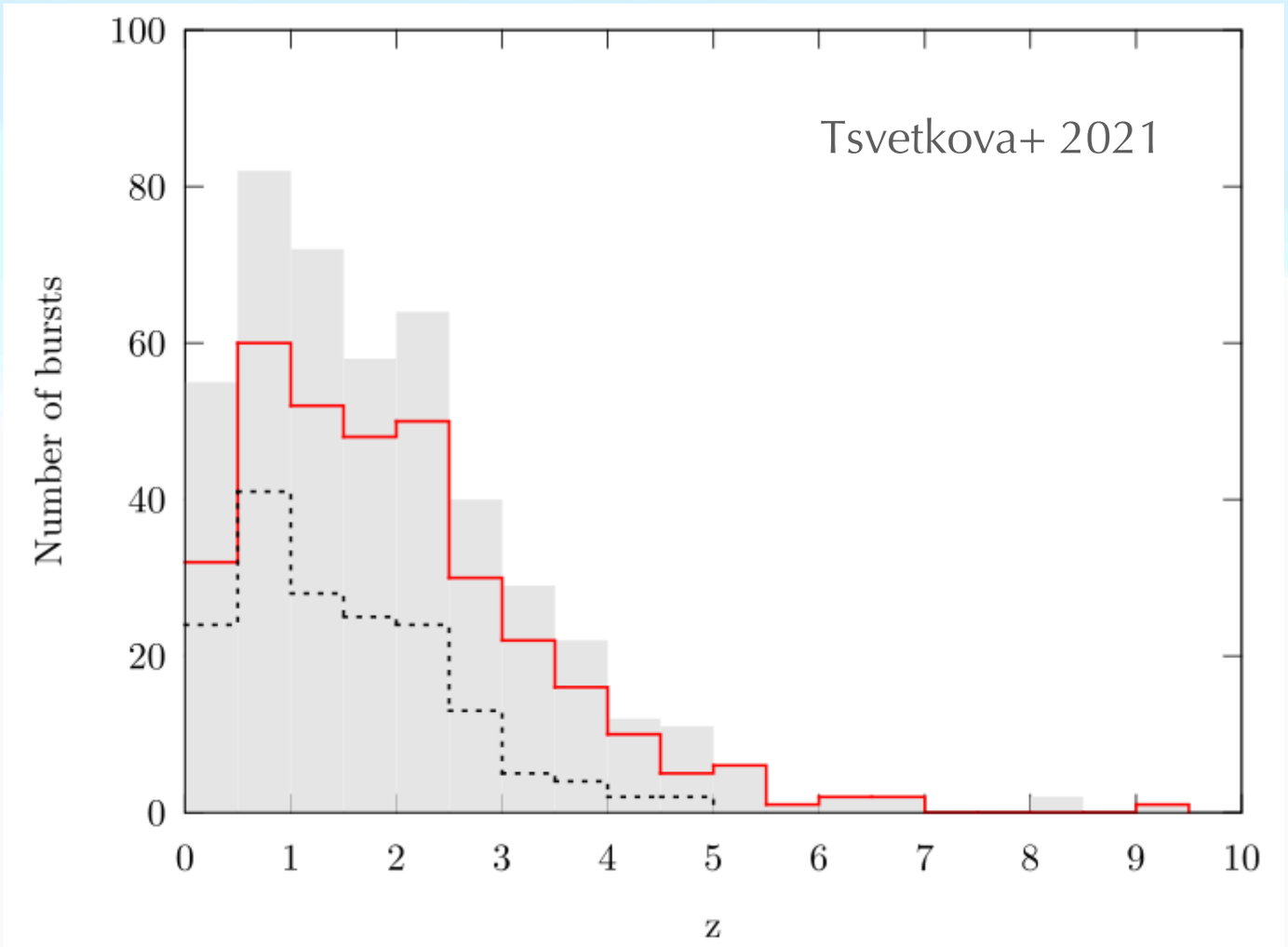

Analysis (triggered sample)

Durations (T100, T90, T50) + spectral lags

↓

Spectral analysis (CPL & Band models)

+ KW LC

↓

Observer-frame energetics (in 10 keV – 10 MeV range)

+ Redshift

↓

Rest-frame energetics

+ Jet break time

↓

Collimation-corrected energetics

Analysis (non-triggered sample)

Targeted search of BAT GRBs with z in the KW waiting-mode LCs: Selection of the TI & peak spectrum accumulation times based on the Bayesian block decomposition of KW LCs and S/N

+ Swift/BAT spectra

Joint spectral analysis of KW+BAT data with CPL and Band functions in the wide 15 keV – 1.5 MeV energy range

+ Swift/BAT LC

Observer-frame energetics

+ Redshift

Rest-frame energetics

+ Jet break time

Collimation-corrected energetics

Hardness-duration distribution

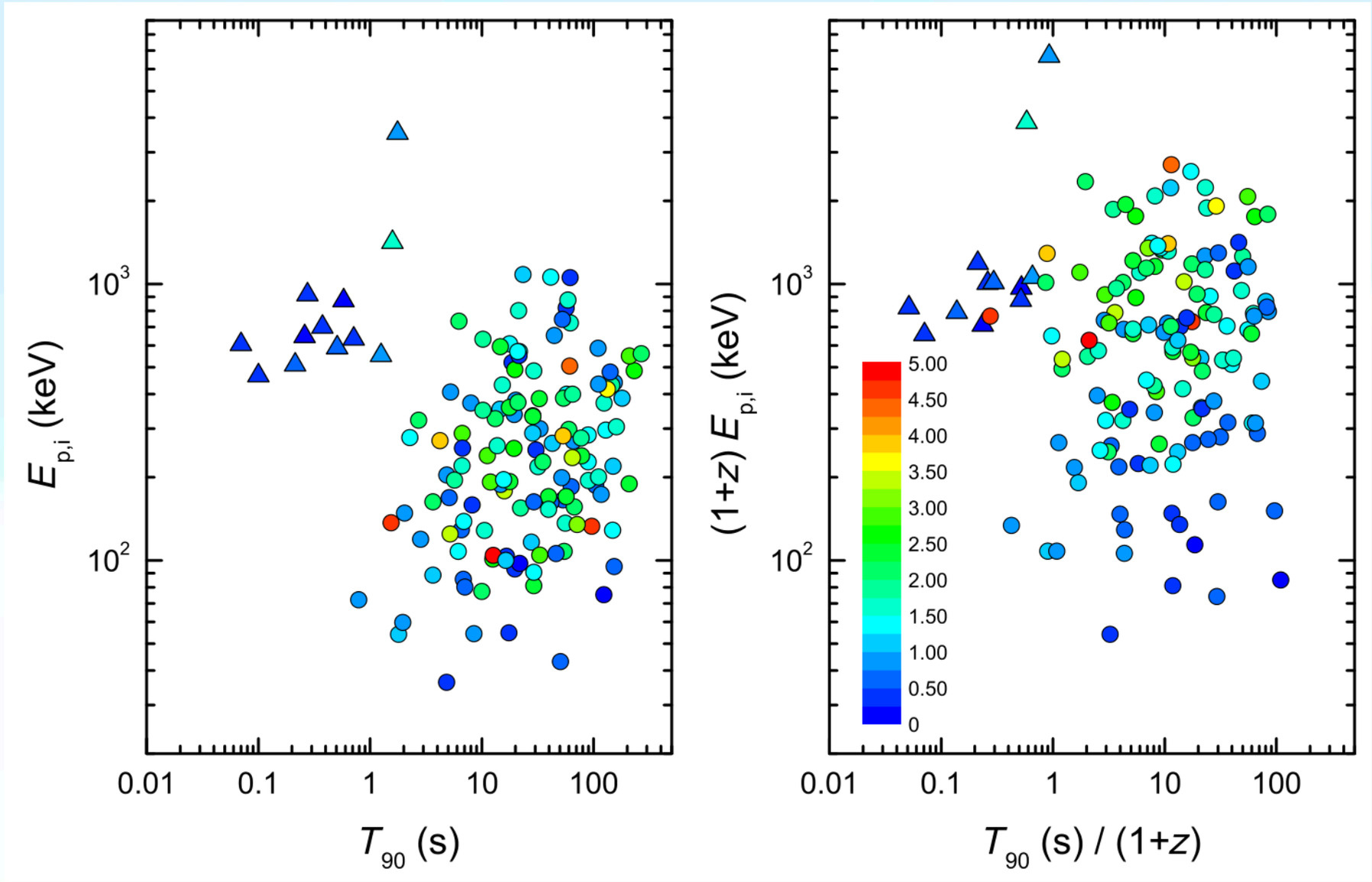

Color mapping: z

Hardness-duration distribution

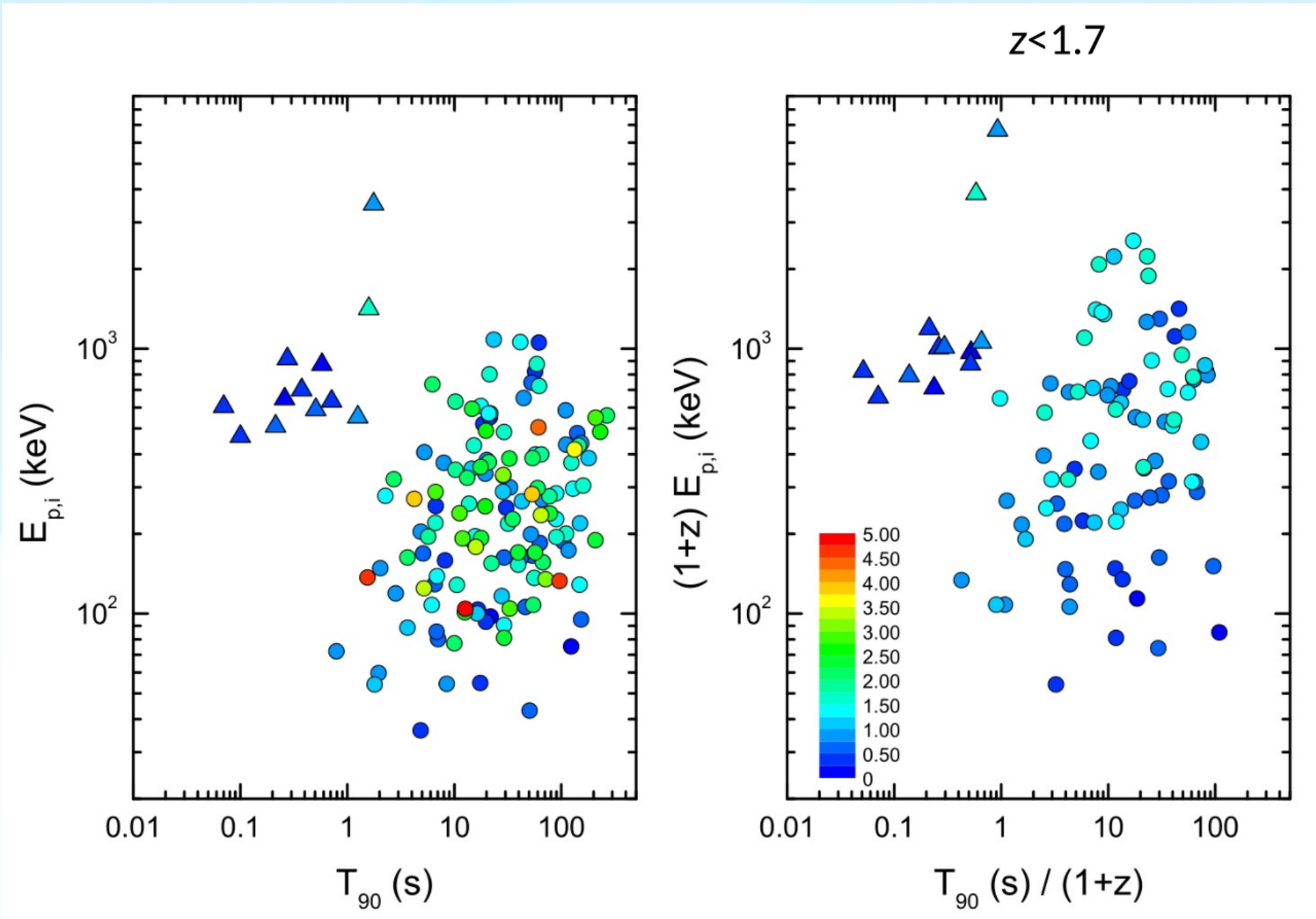

Color mapping: z

Hardness-duration distribution

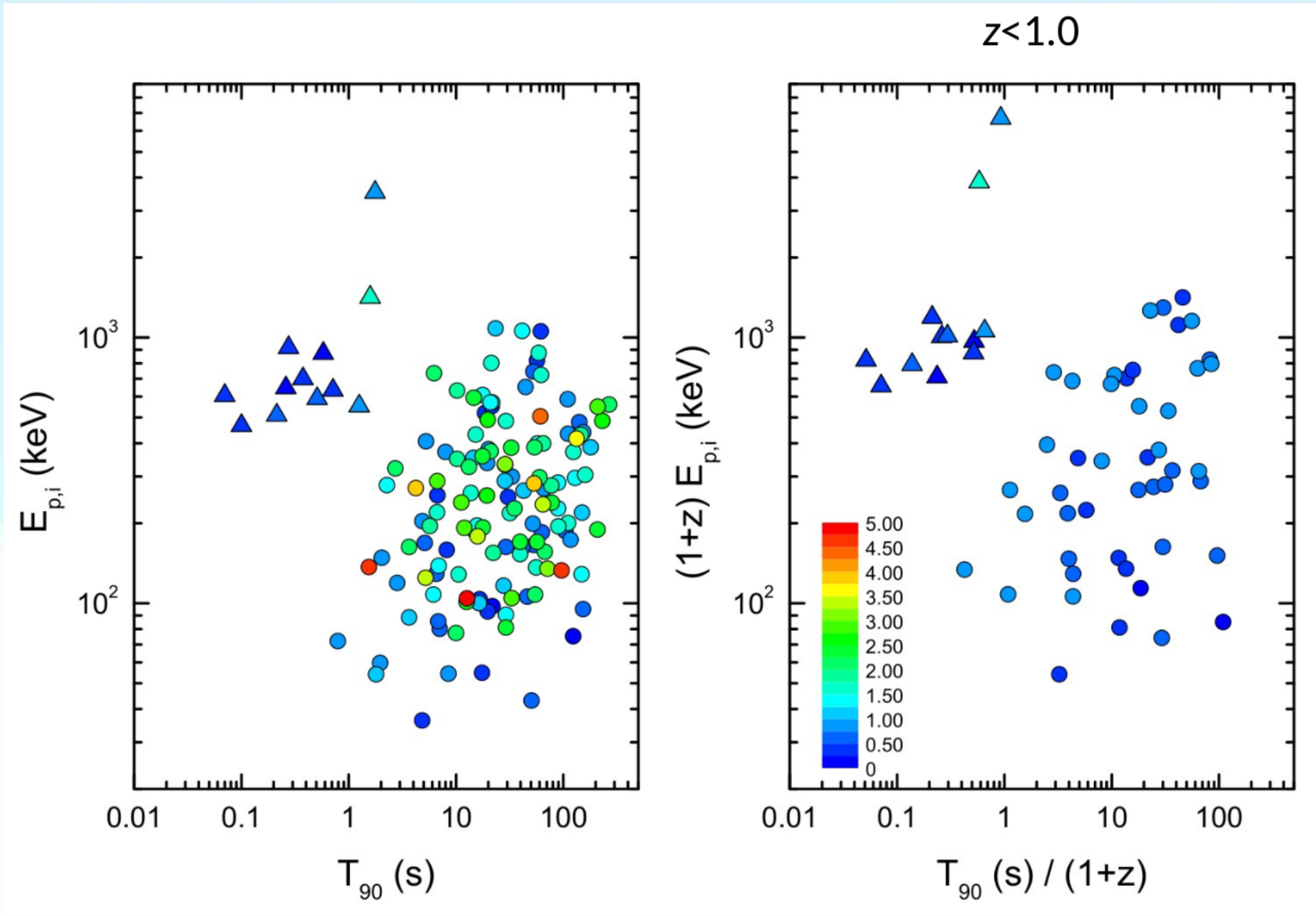

Color mapping: z

Hardness-intensity correlations (T17 + T21)

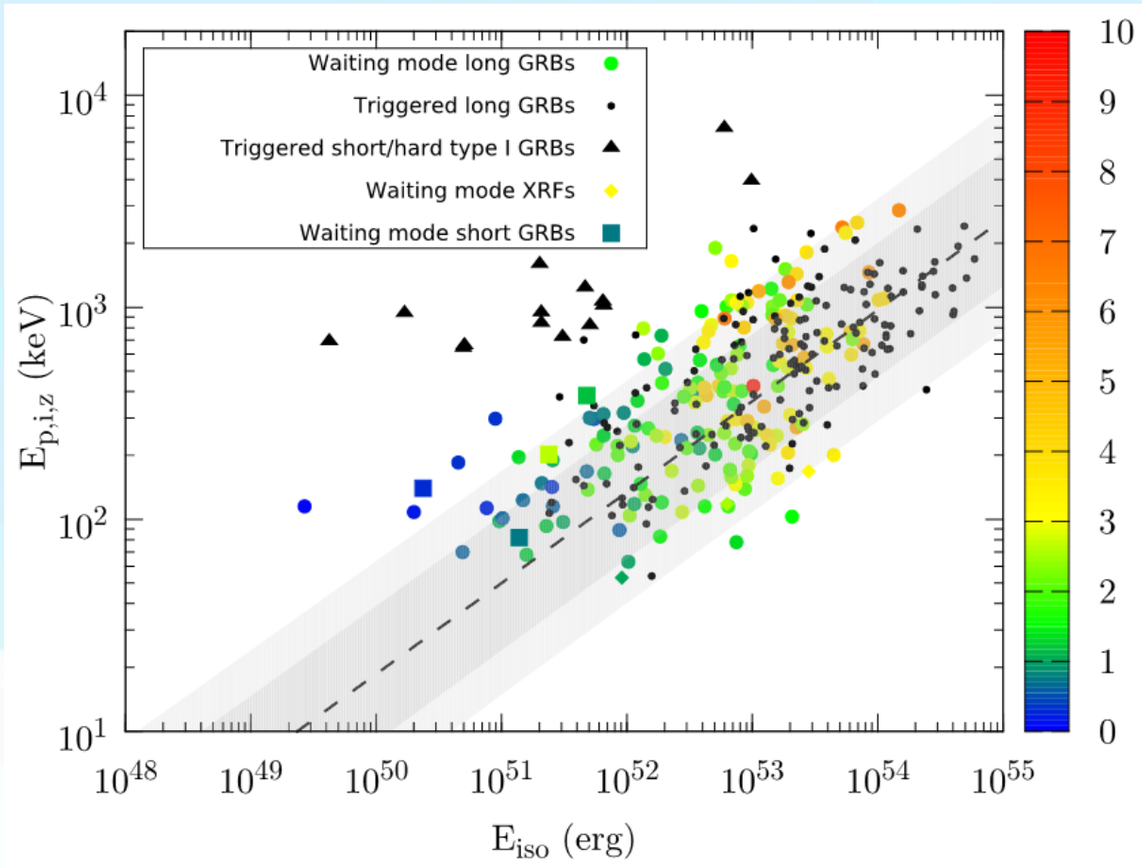

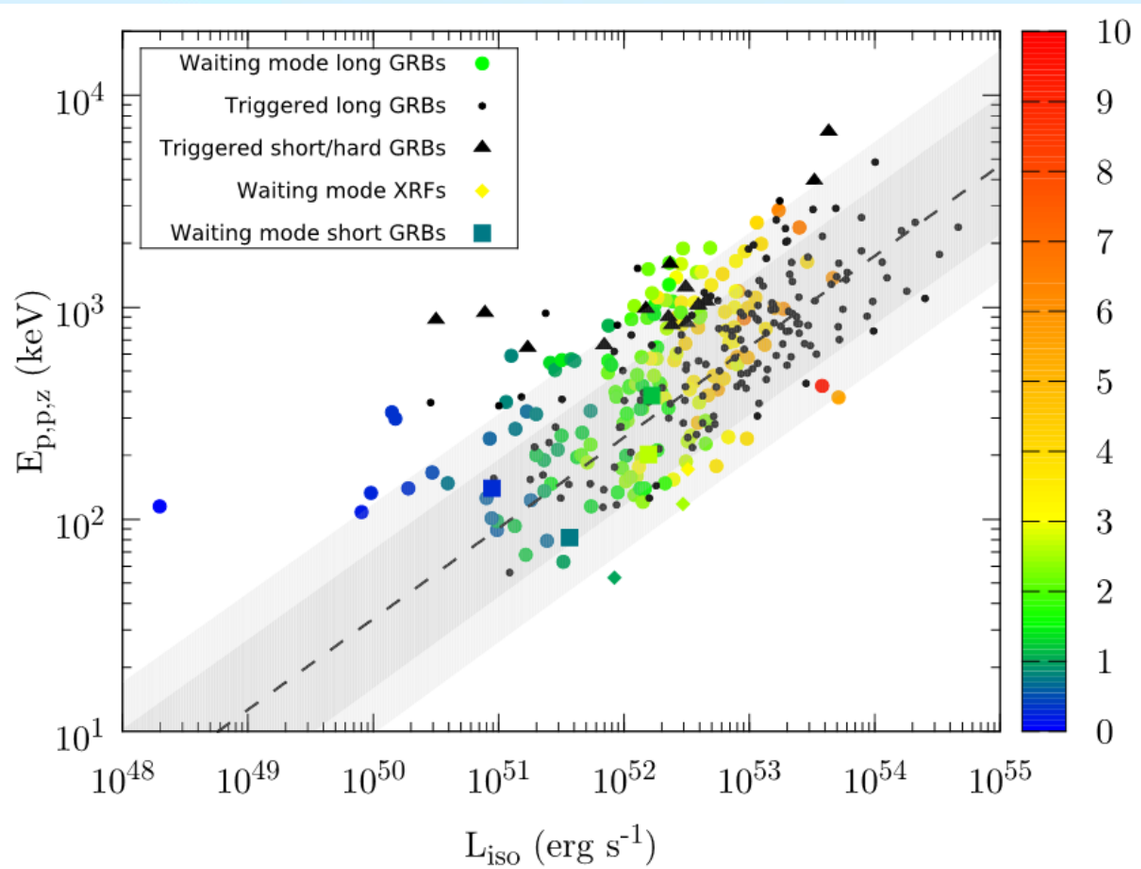

Amati relation
N = 315
ρ_S = 0.7
P < 10^{-5}
slope = 0.36

Color mapping: z

Yonetoku relation
N = 315
ρ_S = 0.7
P < 10^{-5}
slope = 0.40

Hardness-intensity correlations (Type I)

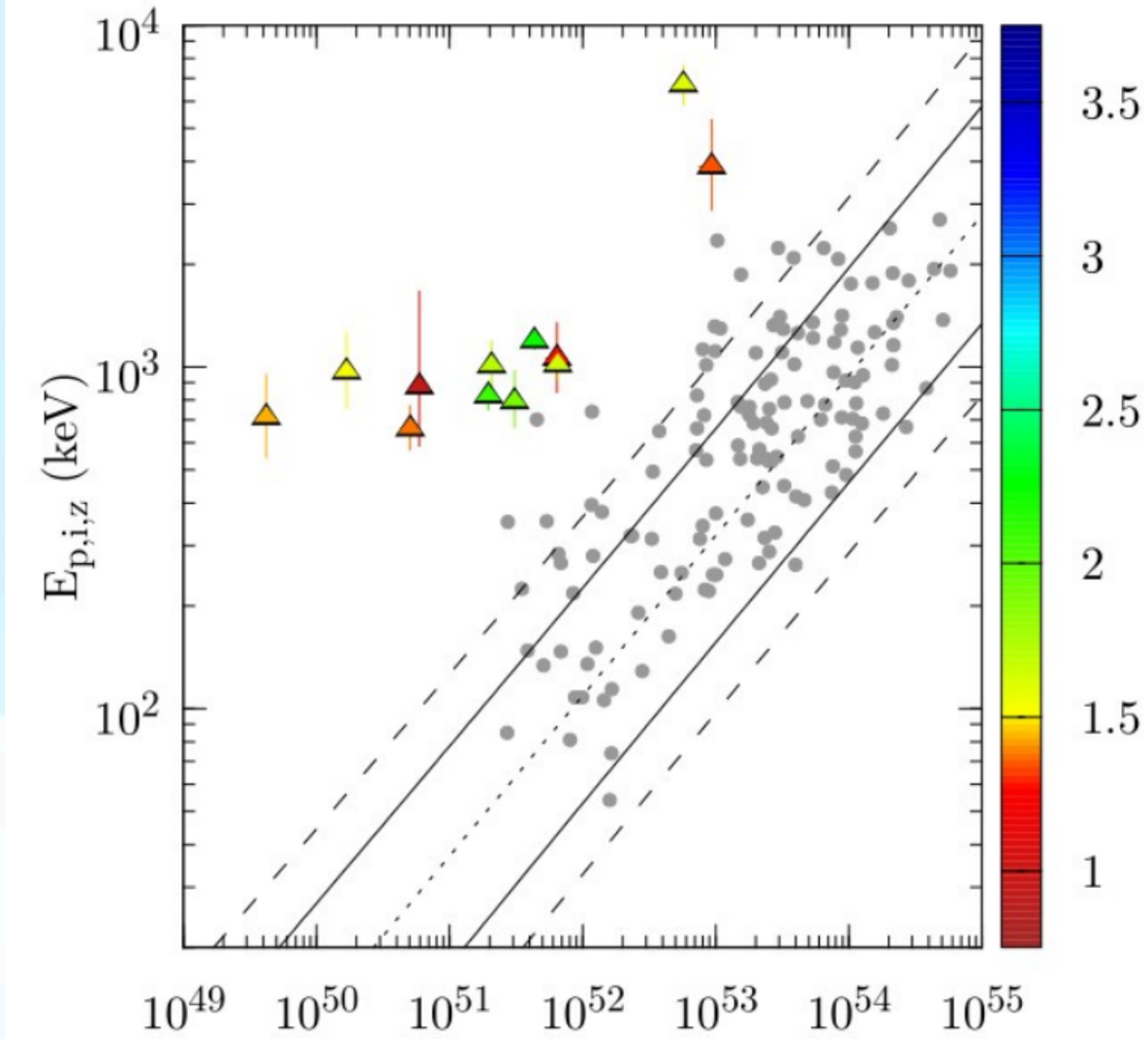

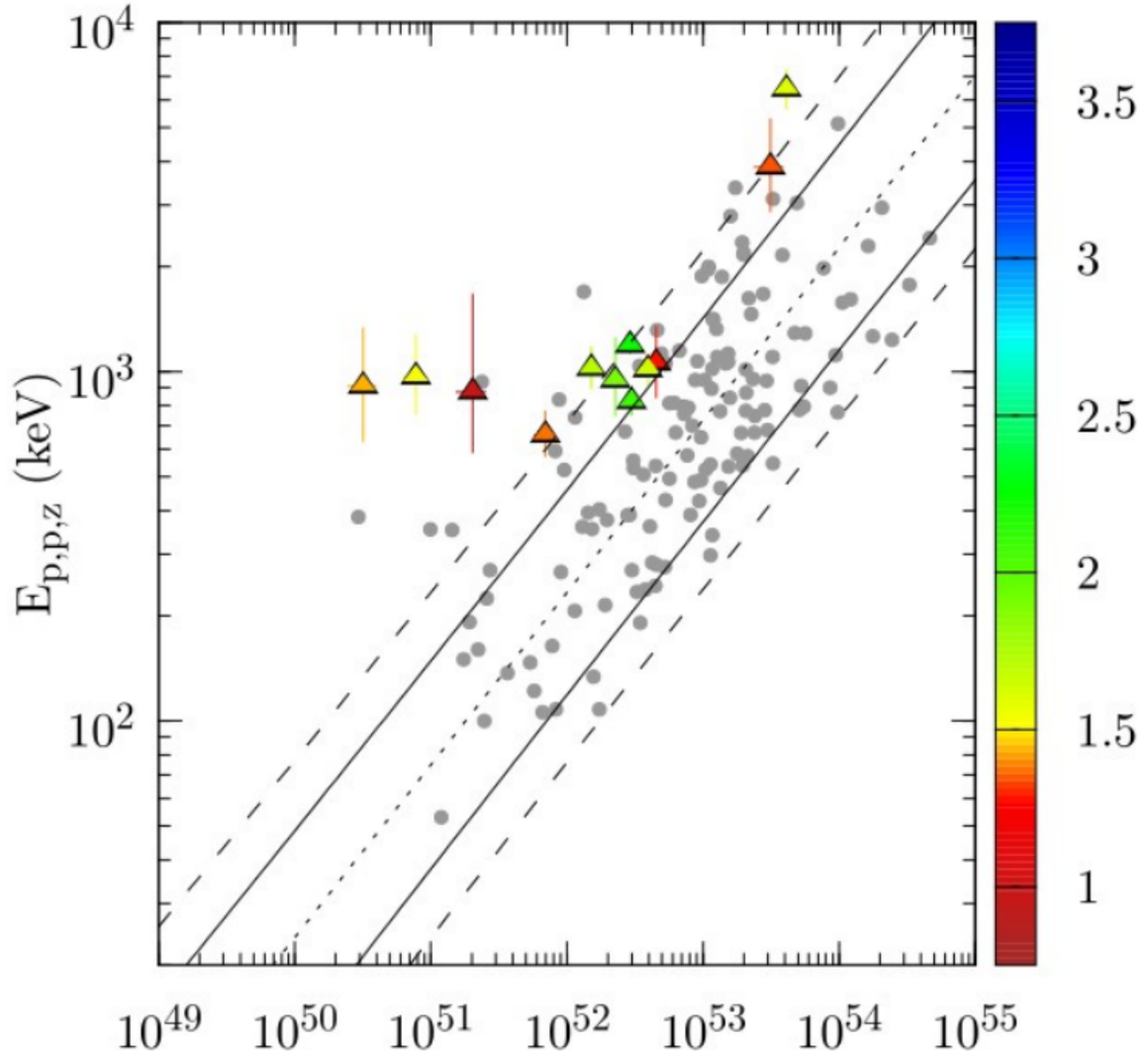

Amati relation
N=12
ρ_S =0.83
P ~ 10^{-3}
a = 0.469

Color mapping:
trigger significance

Yonetoku relation
N=12
ρ_S =0.67
P ~ 1.7 x 10^{-2}
a = 0.494

Collimation-corrected hardness-intensity correlations

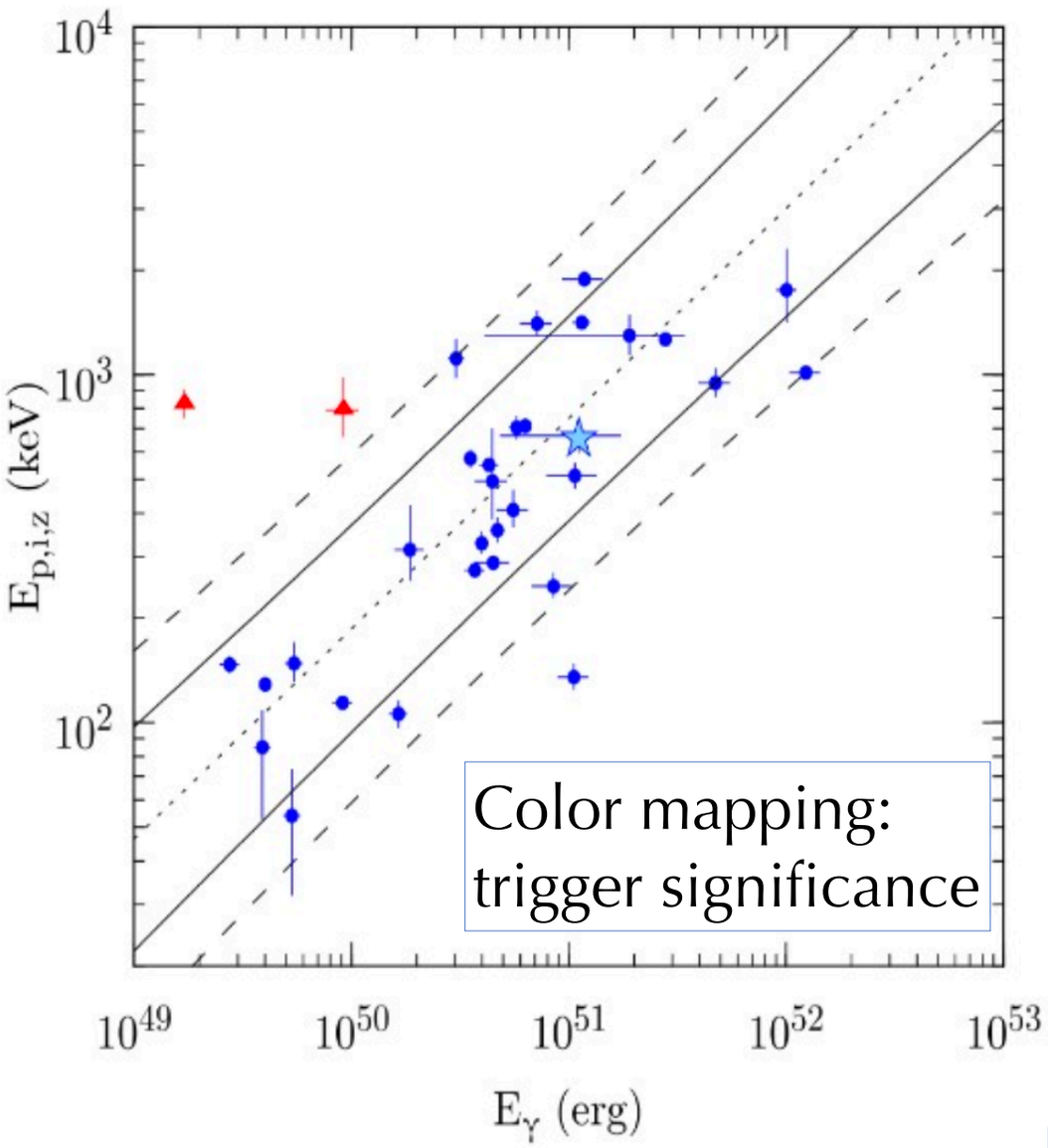

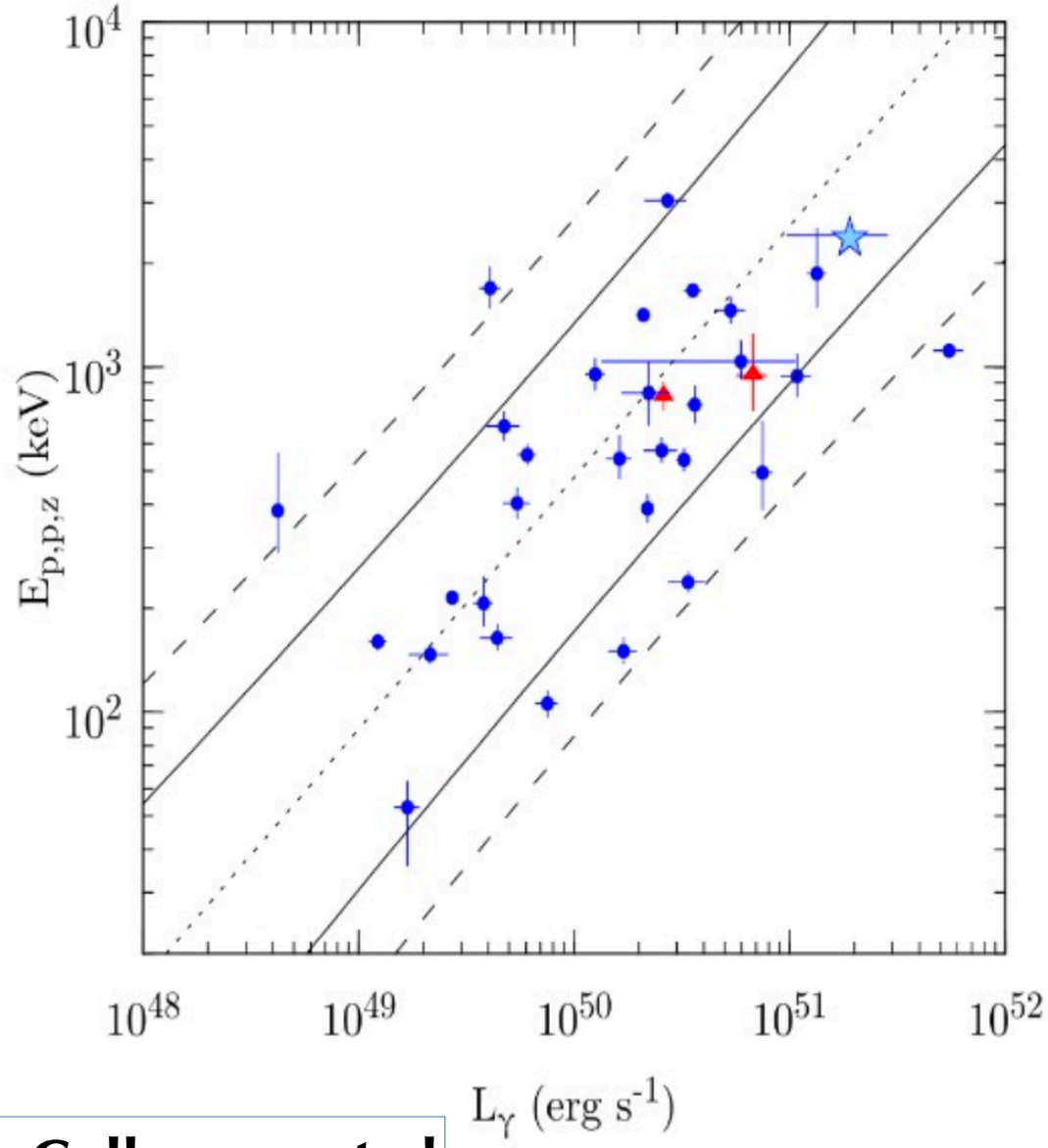

Amati relation
N = 30
ρ_S = 0.80
P = 7.2×10^{-8}
slope = 0.561

Ghirlanda relation
N = 30
ρ_S = 0.77
P = 4.5×10^{-7}
slope = 0.604

Coll.-corrected Yonetoku relation
N=30
ρ_S=0.64
P=9.7×10^{-5}
slope = 0.729

Yonetoku relation
N = 30
ρ_S=0.78
P=2.9×10^{-7} a
slope = 0.496

Selection effects

Trigger threshold (Band 2003):

9σ in G2: ~80 – 300 keV
Solid line: CPL (α= -1)
Dashed line: Band (α= -1, β = -2.5)
Incident angles: 60°

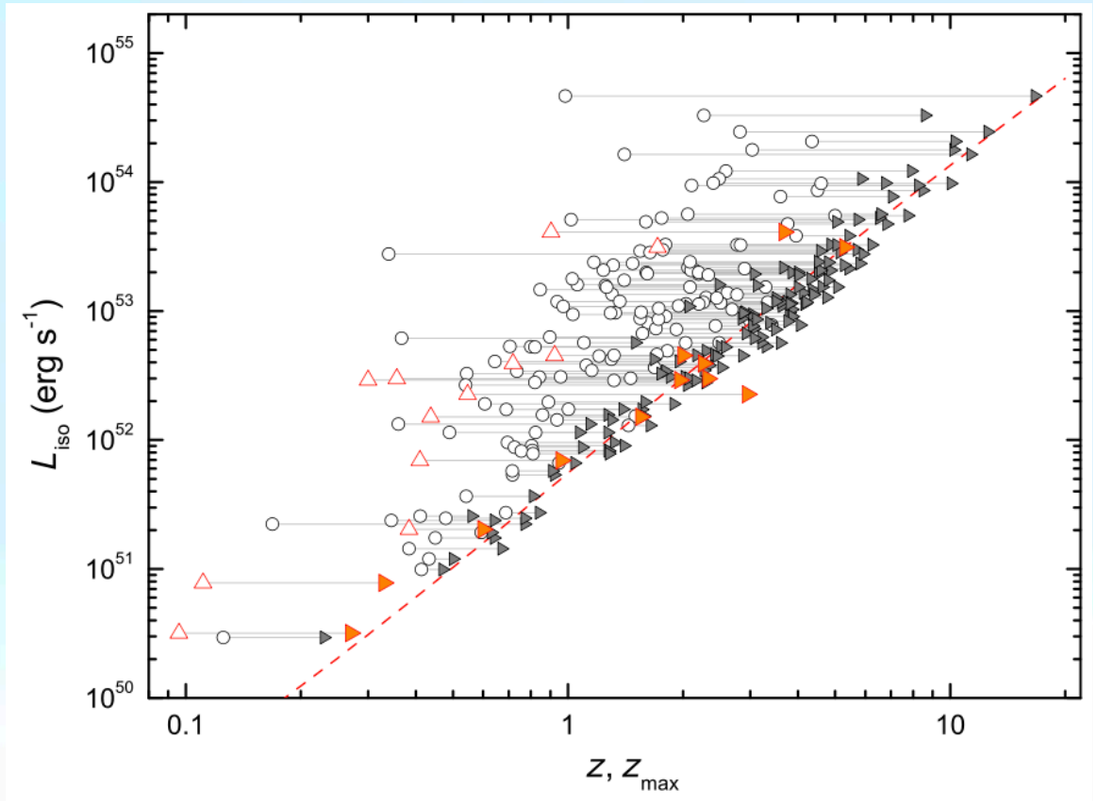

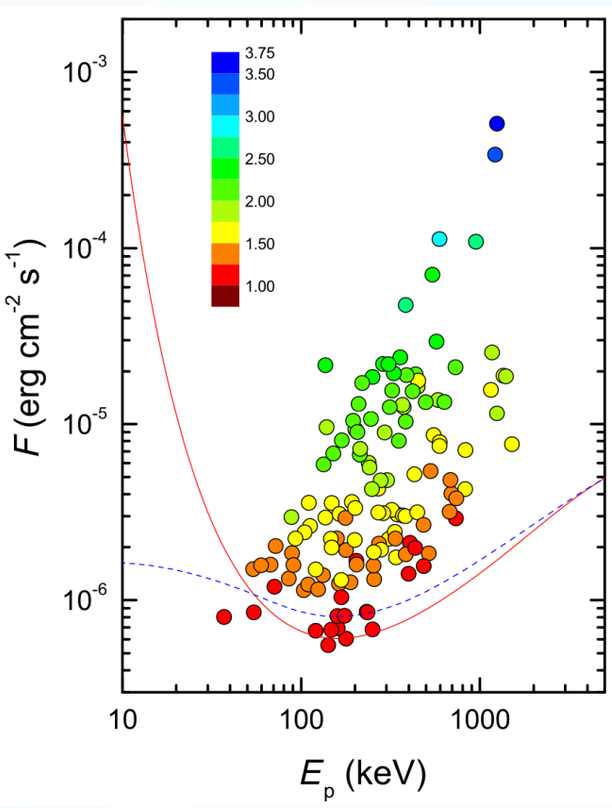

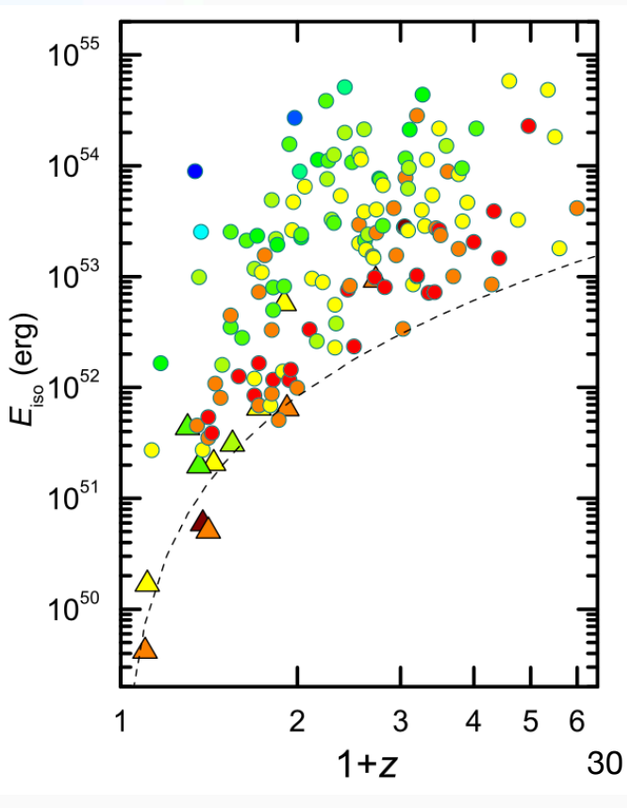

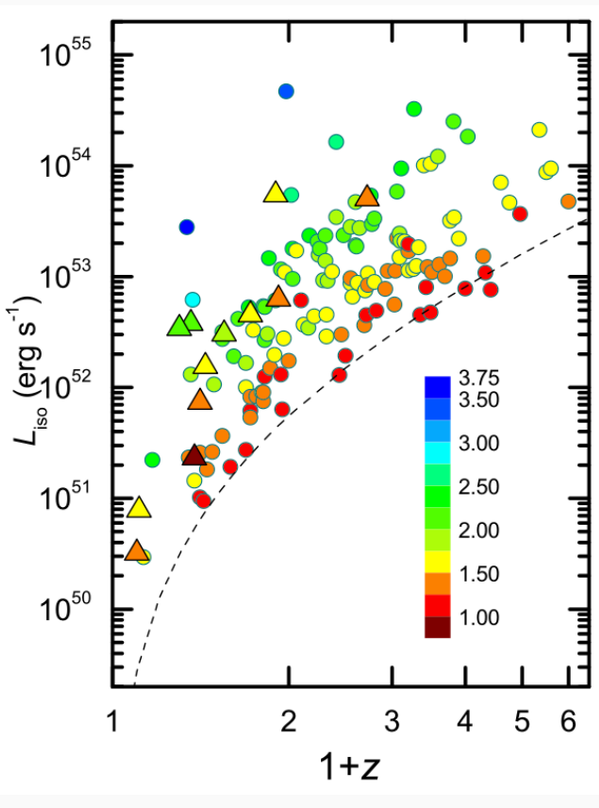

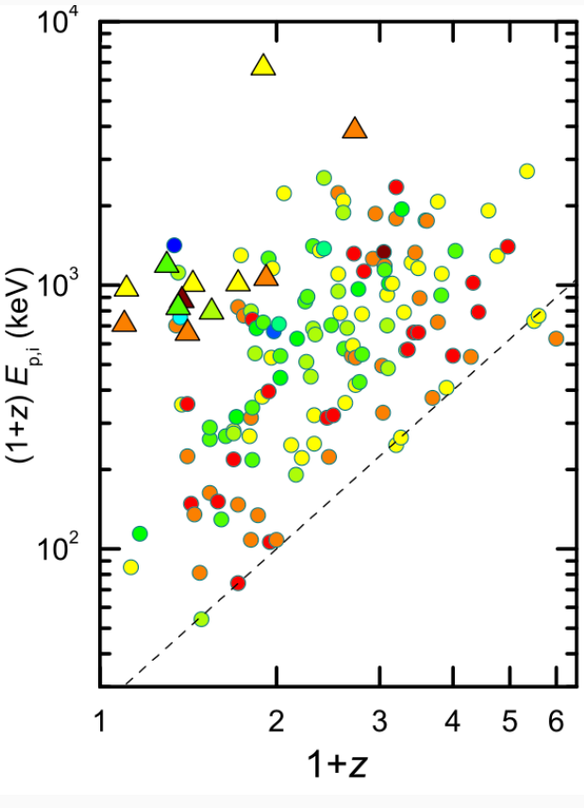

Luminosity and energy release functions

Without loss of generality, the total luminosity function (LF; number of bursts per unit luminosity) $\Phi(L_{iso}, z)$ can be rewritten as

$$\Phi(L_{\rm iso}, z) = \rho(z)\phi(L_{\rm iso}/g(z), \alpha_s)/g(z)$$

$\rho(z)$ – GRB formation rate (GRBFR)

$\phi(L_{\rm iso}/g(z))$ – local LF

$g(z) = (1+z)^{\delta}$ – luminosity evolution (Lloyd-Ronning 2002)

α_s – shape of the LF (Yonetoku 2004)

Examples of evolving astrophysical objects:

• Galaxies: the local luminosity function varies for early- and late-type galaxies (Marzke et al. 1994)

• Quasars: L~(1+z)3, z<1.5 (Boyle 1993; Hewett, Foltz, & Chaffee 1993); L~(1+z)1.5, z<3 (Hewett et al. 1993)

Non-parametric statistical techniques for truncated data samples

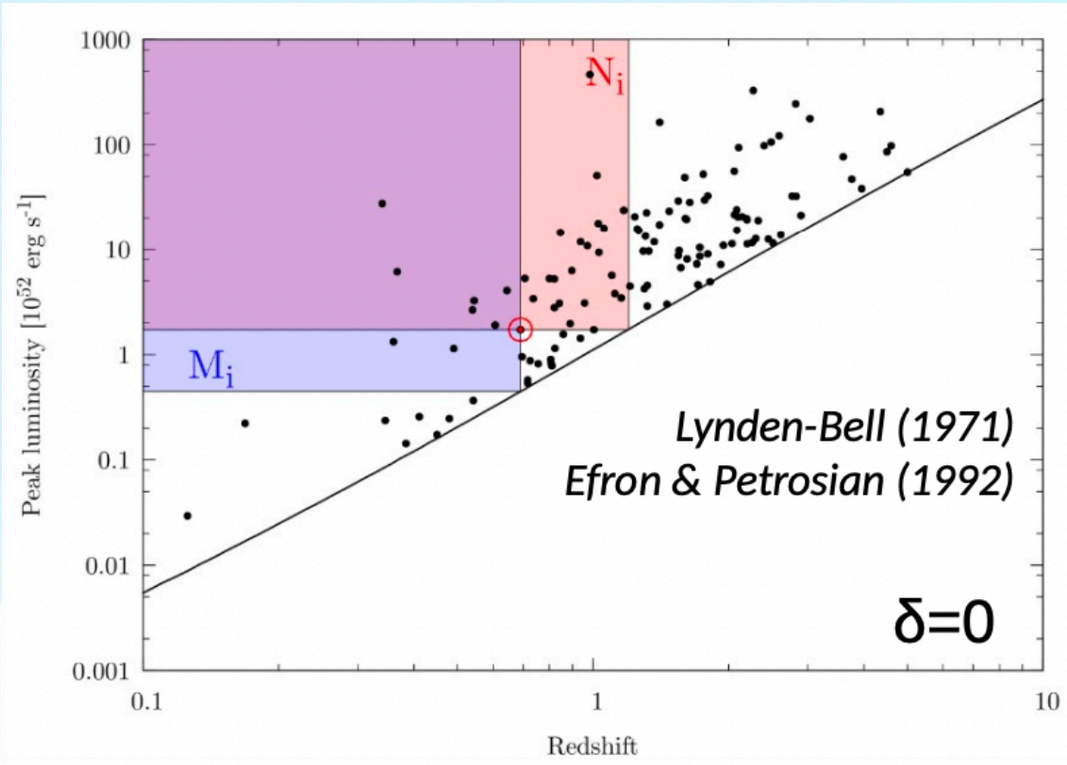

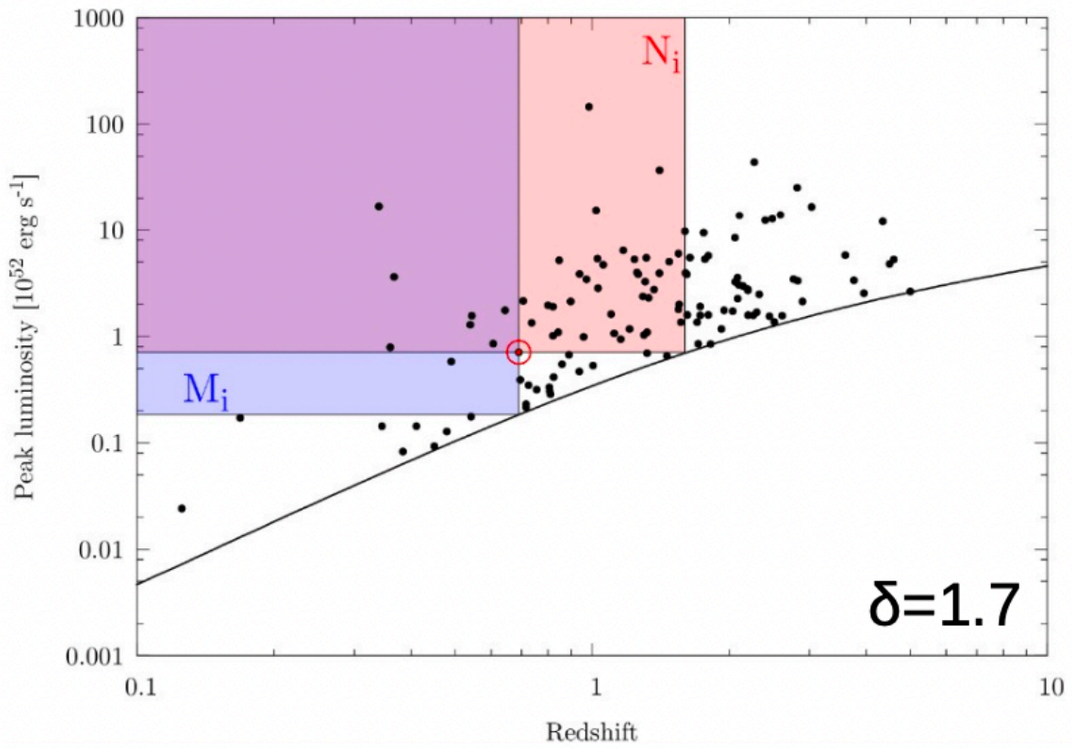

Associated sets:

M_i: $J'_i = \{j | z_j < z_i, L_j > L_{\rm lim,i}, L_{\rm i} > L_{\rm lim,j}\}$

$$L_j > L_i^{\rm lim} \Leftrightarrow z_j^{\rm lim} > z_i$$

N_i: $J_i = \{j | L_j > L_i, L_i > L_{\rm lim,j}\}$

$$\Updownarrow$$

$$J_i = \{j | L_j > L_i, z_j < z_{\rm lim,i}\}$$

Cumulative GRB number

$$\ln \psi(z_i) = \sum_{j=2}^{i} \ln\left(1 + \frac{1}{M_j}\right)$$

Cumulative LF

$$\ln \psi(L'_i) = \sum_{j=2}^{i} \ln\left(1 + \frac{1}{N'_j}\right)$$

Non-parametric statistical techniques for truncated data samples

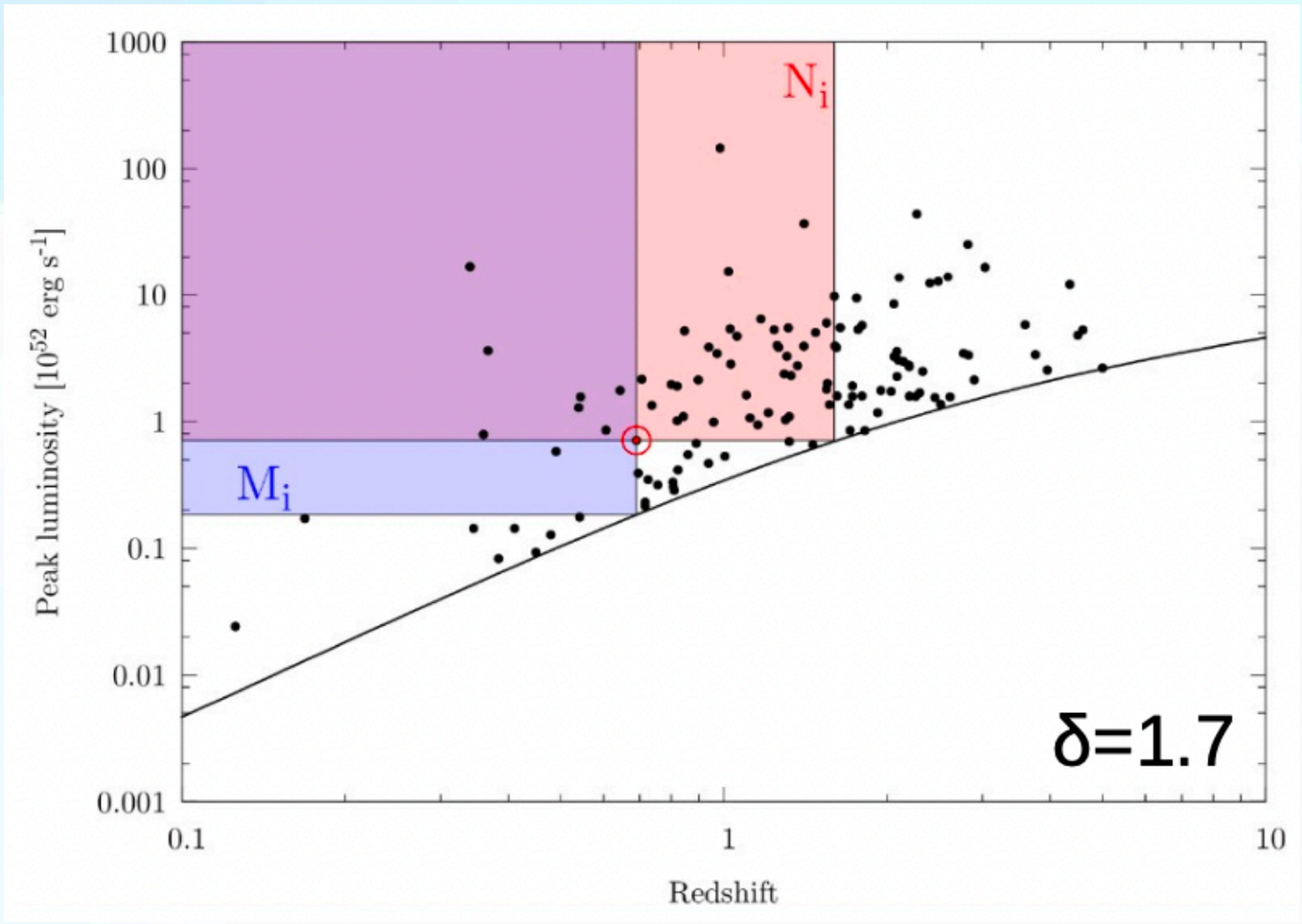

$$\tau = \frac{\sum_i (R_i - E_i)}{\sqrt{\sum_i V_i}}$$

$$E_i = (N_i + 1)/2$$

$$V_i = (N_i^2 - 1)/12$$

Luminosity evolution

$$g(z) = (1+z)^{\delta}$$

Local (non-evolving) luminosity

$$L' = L/g(z)$$

Local LF (in the commoving frame)

$$\psi(L')(1+z)^{\delta_L}$$

Luminosity and energy release evolution (T17)

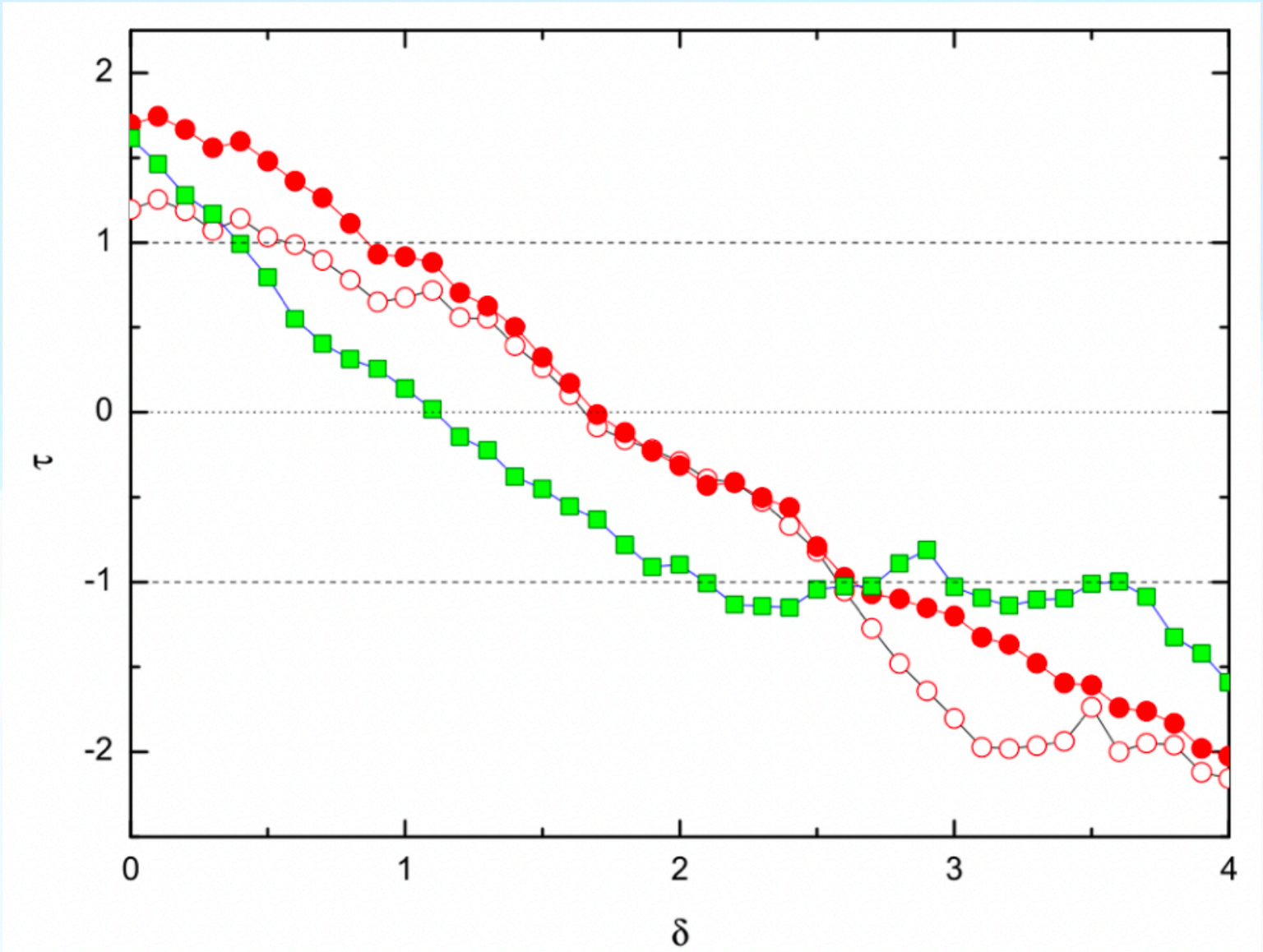

Liso: τ_0 =1.7 σ

Eiso: τ_0 =1.6 σ

GRBs might be brighter in the past

Red filled circles : per-burst truncation flux $F_{lim,i}$

red open circles: monolithic $F_{lim} = 2\times10^{-6}$ erg cm^{-2} s^{-1}

green squares: $S_{lim} = 4.3 \times 10^{-6}$ erg cm^{-2}

LF, EF, GRBFR

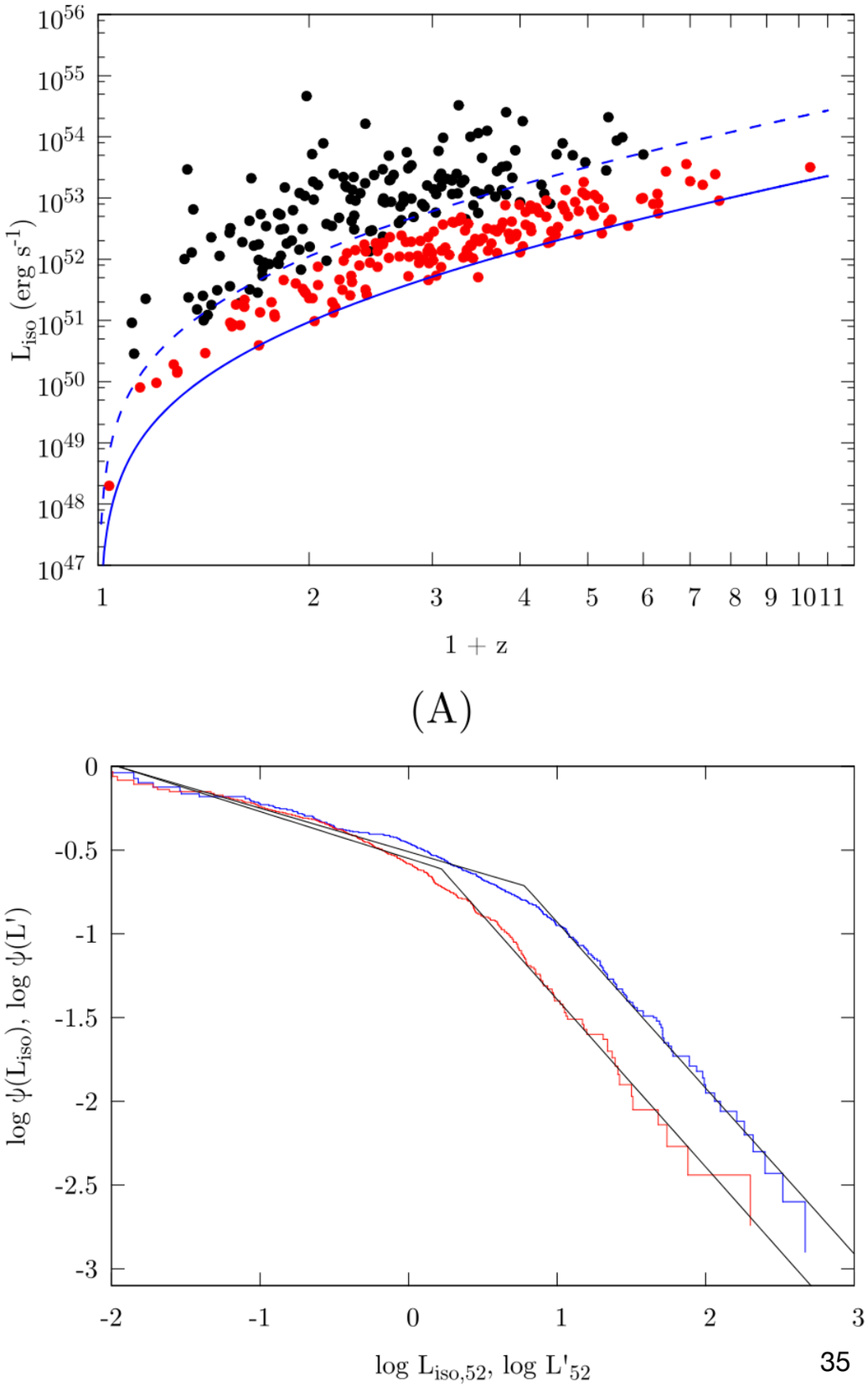
L_{iso} (erg s^{-1})
1 + z
(A)
log $\psi(L_{iso})$, log $\psi(L')$
log $L_{iso,52}$, log L'_{52}

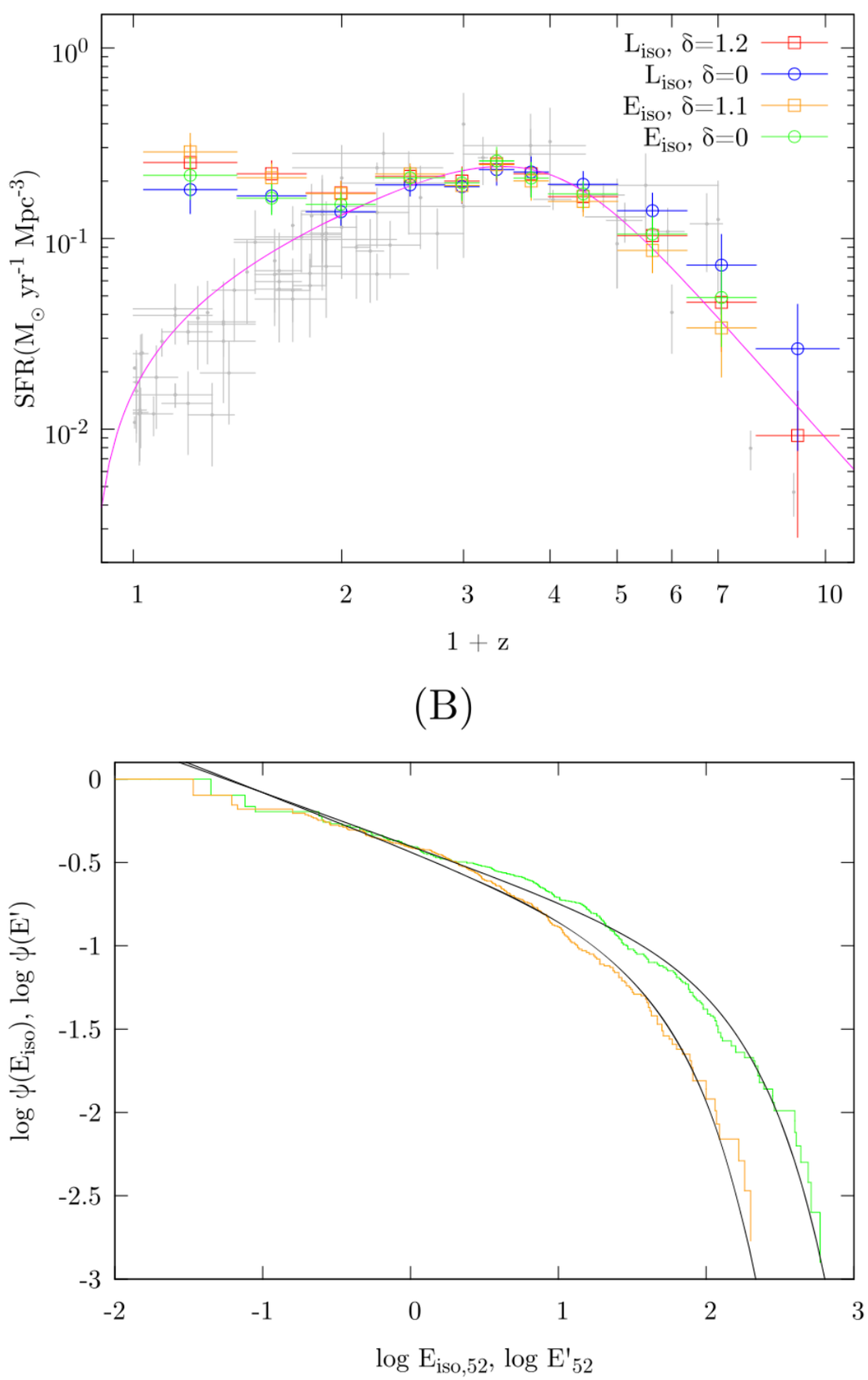
L_{iso}, δ=1.2
L_{iso}, δ=0
E_{iso}, δ=1.1
E_{iso}, δ=0
SFR($M_\odot$ yr^{-1} Mpc^{-3})
1 + z
(B)
log $\psi(E_{iso})$, log $\psi(E')$
log $E_{iso,52}$, log E'_{52}

Sample	Number of bursts
"KW trig"	193
"KW & BAT"	167
"GBM only"	49
"GBM all"	168
"Total"	409

Clustering of GRBs in their rest-frame

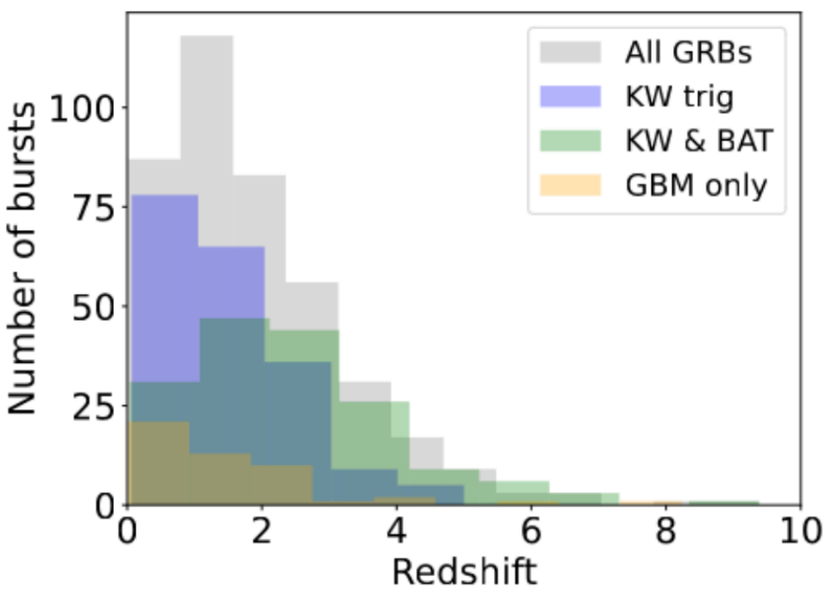

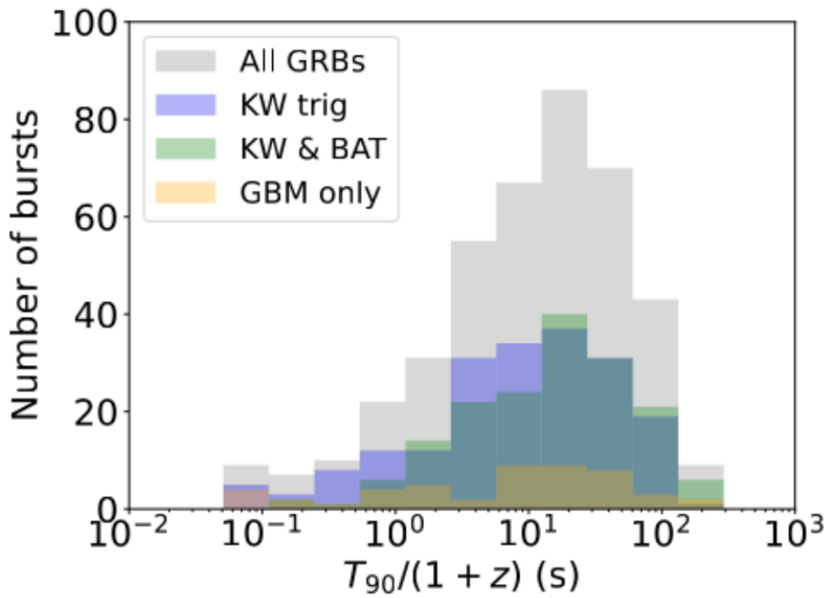

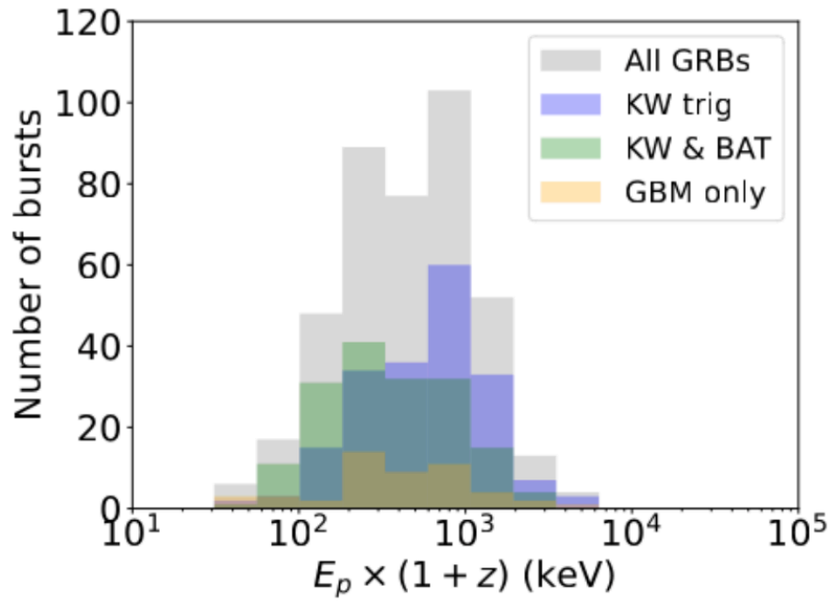

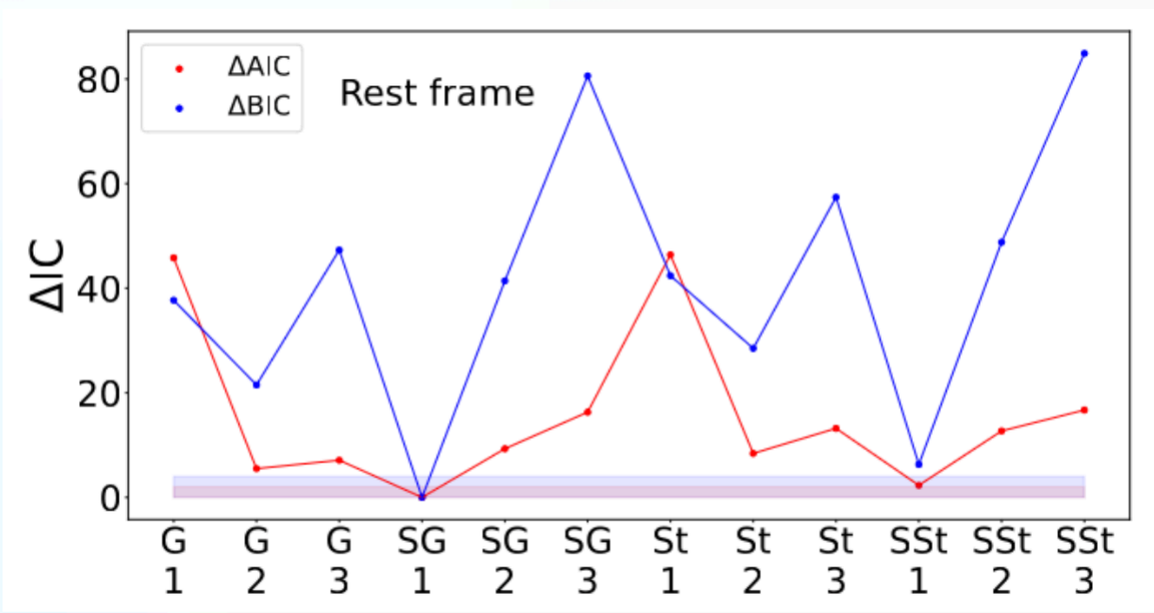

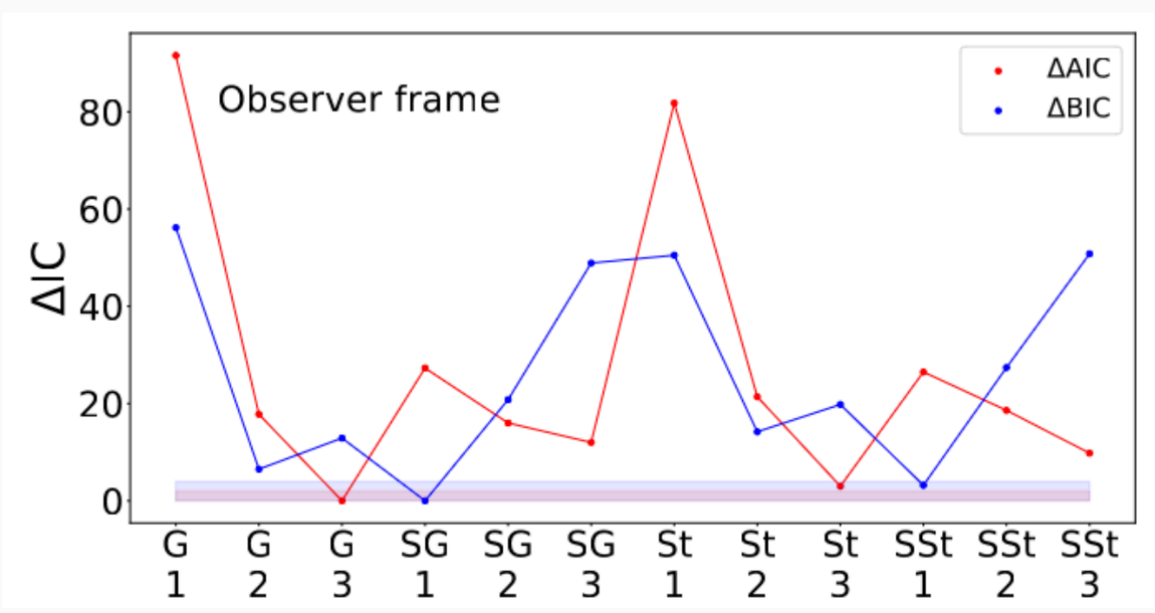

Modeling of GRB light curves

Boris E. Stern and
Roland Svensson
ApJ 469:L109 (1996)

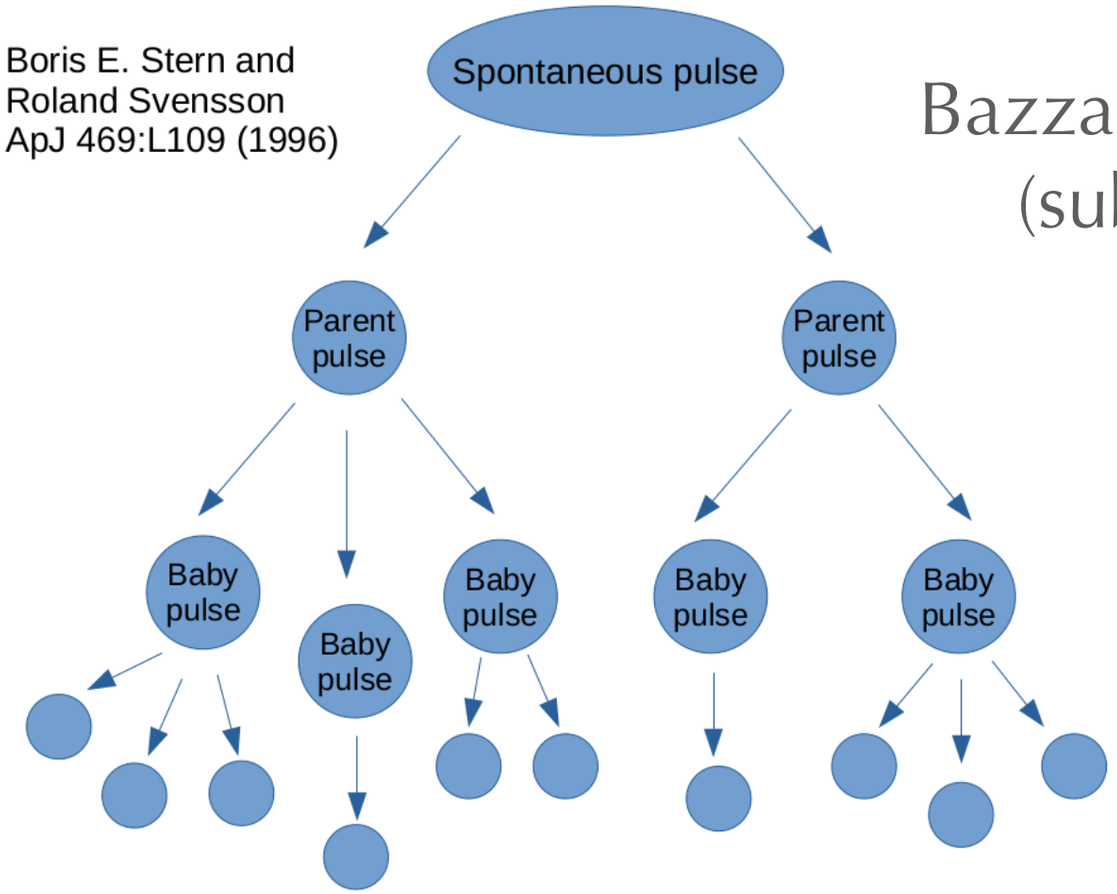

Bazzanini+ 2024
(submitted)

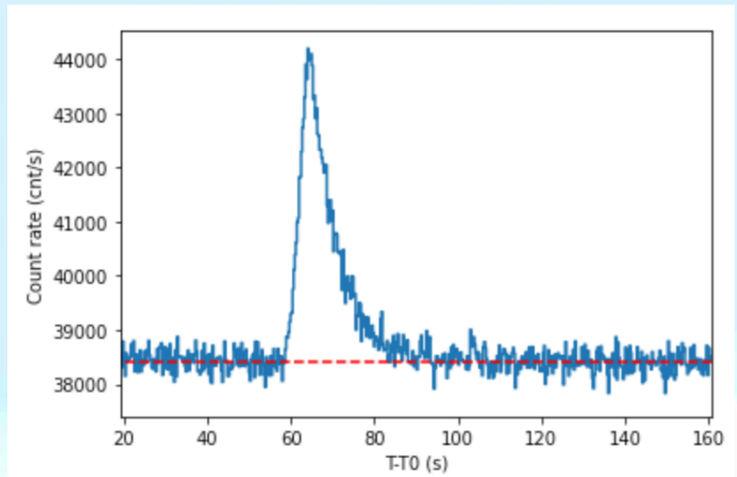

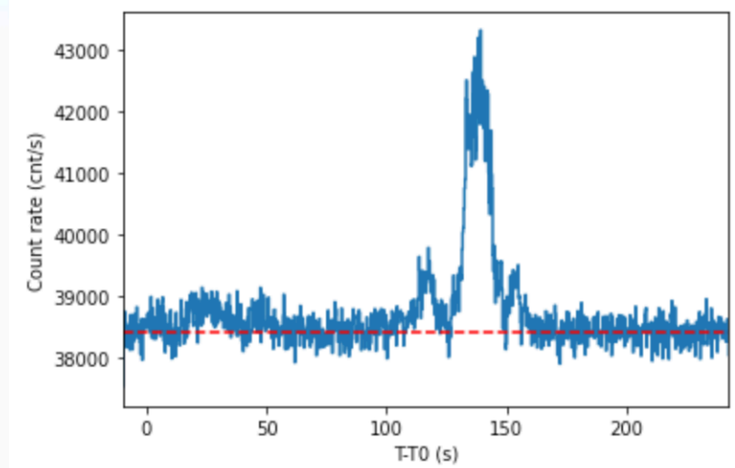

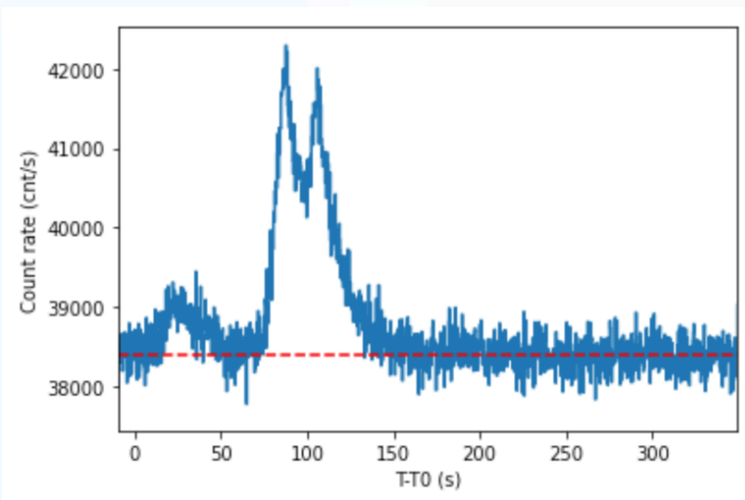

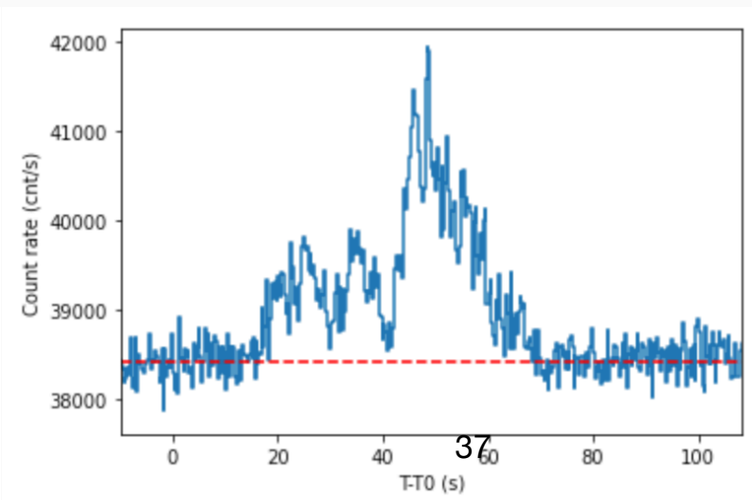

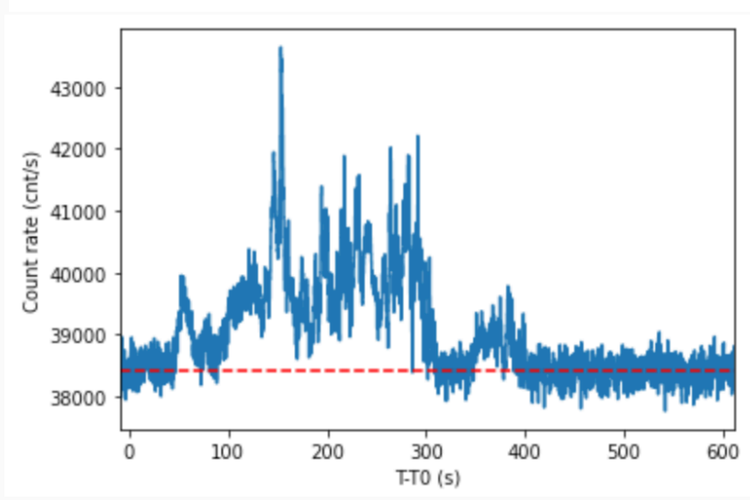

A concept of assessment of LIV tests with *THESEUS* using the GRBs detected by *Fermi*/GBM

Tsvetkova+ 2023

$$\tau_{\mathrm{total,\,obs}}(E_{\mathrm{rf}},z) = \tau_{\mathrm{int,\,obs}}(E_{\mathrm{rf}}) + \xi\left(\frac{1}{H_0}\right)\left(\frac{E_{\mathrm{rf}}}{\zeta E_{\mathrm{pl}}}\right)^n\left(\frac{1+n}{2}\right)\left(\frac{1}{1+z}\right)^n\int_0^z \frac{(1+z')^n dz'}{\sqrt{\Omega_m(1+z')^3+\Omega_\Lambda}}.$$

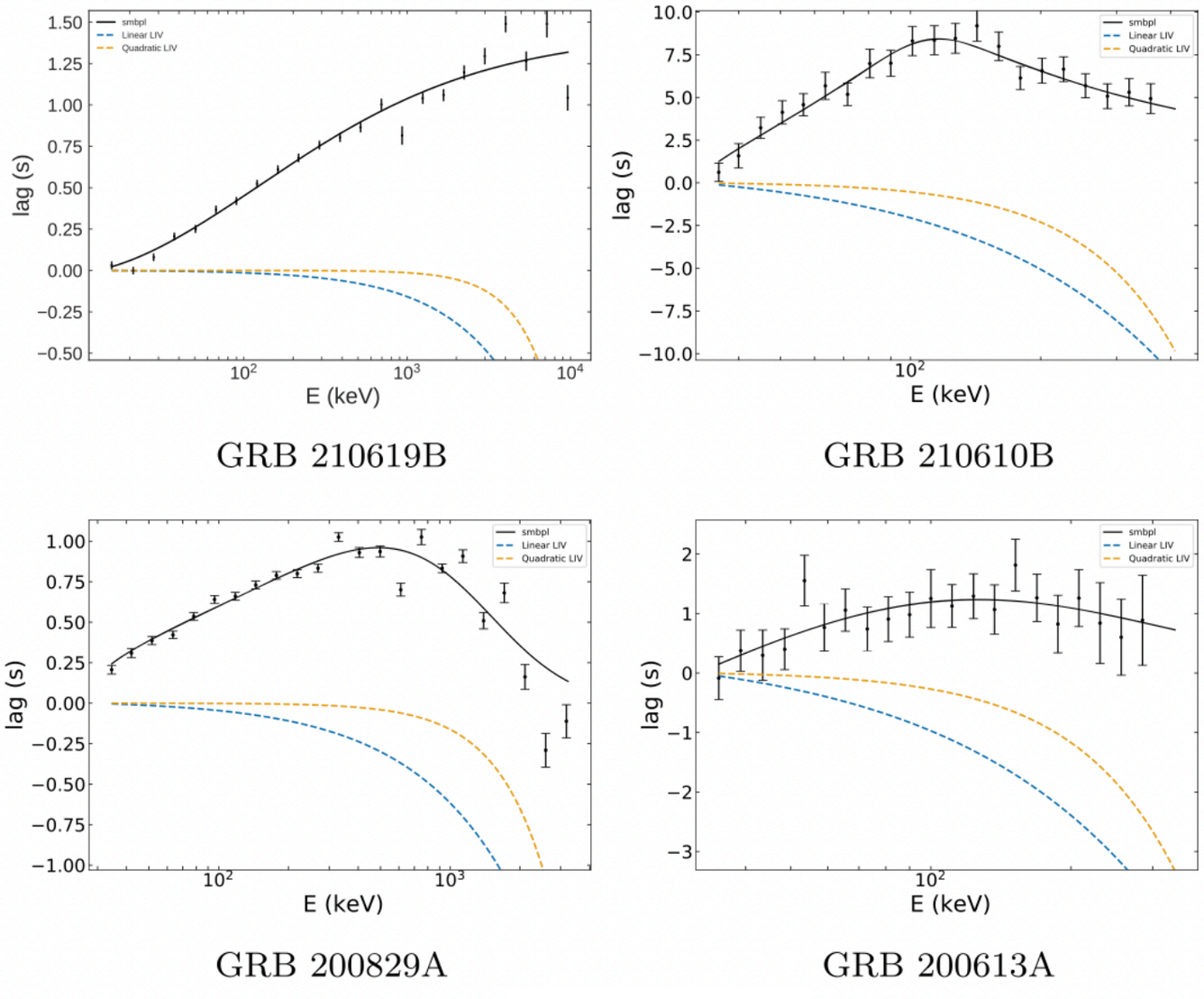

GRB 210619B

GRB 210610B

GRB 200829A

GRB 200613A

Liu+ 2022

$$v_{\mathrm{phot}}/c - 1 = \xi\left(\frac{E_{\mathrm{obs}}}{E_{\mathrm{QG}}}\right)^n,$$

Thank you for your attention!